2.実用新案登録　特になし

3.その他　特になし

IV　研究成果の刊行に関する一覧表

雑誌　（主なものを３つ選んで掲載）

発表者氏名	論文タイトル名	発表誌名	巻号	ページ	出版年
Yamazoe T, Shiraki N, Toyoda M, Kiyokawa N, Okita H, Miyagawa Y, Akutsu H, Umezawa A, Sasaki Y, Kume K, Kume S.	A synthetic nanofibrillar matrix promotes in vitro hepatic differentiation of embryonic stem cells and induced pluripotent stem cells	Journal of Cell Science	26(Pt23)	5391-5399	2013
Sasai N, Saitoh N, Saitoh H, Nakao M	The transcriptional cofactor MCAF1/ATF7IP is involved in histone gene expression and cellular senescence.	PLoS One	8(7)	e68478	2013
Iwashita H, shiraki N, Sakano D, IkegaShiga M, Kume K, Kume S.	Secreted cerberus1 as a marker for quantification of definitive endoderm differentiation of the pluripotent stem cells.	PLoS One	8(5)	e64291	2013

V　研究成果の刊行物・別刷

A synthetic nanofibrillar matrix promotes *in vitro* hepatic differentiation of embryonic stem cells and induced pluripotent stem cells

Taiji Yamazoe[1,2,3], Nobuaki Shiraki[1], Masashi Toyoda[4], Nobutaka Kiyokawa[4], Hajime Okita[4], Yoshitaka Miyagawa[4], Hidenori Akutsu[4], Akihiro Umezawa[4], Yutaka Sasaki[2], Kazuhiko Kume[1] and Shoen Kume[1,3,5,*]

[1]Division of Stem Cell Biology, Institute of Molecular Embryology and Genetics, Kumamoto University, Honjo 2-2-1, Kumamoto 860-0811, Japan
[2]Department of Gastroenterology and Hepatology, Faculty of Life Science, Kumamoto University, Honjo 2-2-1, Kumamoto 860-0811, Japan
[3]G.COE, Kumamoto University, Honjo 2-2-1, Kumamoto 860-0811, Japan
[4]Department of Reproductive Biology, National Institute for Child Health and Development, Okura 2-10-1, Setagaya, Tokyo 157-8535, Japan
[5]Program for Leading Graduate Schools 'HIGO (Health life science; Interdisciplinary and Glocal Oriented) Program', Kumamoto University, Honjo 221, Chuoku, Kumamoto 8600811, Japan
*Author for correspondence (skume@kumamoto-u.ac.jp)

Accepted 9 September 2013
Journal of Cell Science 126, 5391–5399

doi: 10.1242/jcs.129767

Summary

Embryonic stem (ES) cells recapitulate normal developmental processes and serve as an attractive source for routine access to a large number of cells for research and therapies. We previously reported that ES cells cultured on M15 cells, or a synthesized basement membrane (sBM) substratum, efficiently differentiated into an endodermal fate and subsequently adopted fates of various digestive organs, such as the pancreas and liver. Here, we established a novel hepatic differentiation procedure using the synthetic nanofiber (sNF) as a cell culture scaffold. We first compared endoderm induction and hepatic differentiation between murine ES cells grown on sNF and several other substrata. The functional assays for hepatocytes reveal that the ES cells grown on sNF were directed into hepatic differentiation. To clarify the mechanisms for the promotion of ES cell differentiation in the sNF system, we focused on the function of Rac1, which is a Rho family member protein known to regulate the actin cytoskeleton. We observed the activation of Rac1 in undifferentiated and differentiated ES cells cultured on sNF plates, but not in those cultured on normal plastic plates. We also show that inhibition of Rac1 blocked the potentiating effects of sNF on endoderm and hepatic differentiation throughout the whole differentiation stages. Taken together, our results suggest that morphological changes result in cellular differentiation controlled by Rac1 activation, and that motility is not only the consequence, but is also able to trigger differentiation. In conclusion, we believe that sNF is a promising material that might contribute to tissue engineering and drug delivery.

Key words: Hepatic differentiation, *In vitro* differentiation, Embryonic stem cells, Induced pluripotent stem cells

Introduction

The liver is an important organ that performs many complex functions, including the metabolism of carbohydrates, proteins and lipids, as well as storage of essential nutrients and biotransformation of drugs. Drug biotransformation involves detoxification and bioactivation, where the metabolite becomes more toxic. Therefore, drug biotransformation plays an important role in the early stages of drug discovery processes. Primary hepatocyte cultures are often used for pharmacological assays, but they are short-lived and cannot be maintained in long-term culture. In addition, there are considerable donor-dependent variations. By contrast, embryonic stem (ES) cells or induced pluripotent stem (iPS) cells can proliferate infinitely and maintain their pluripotent ability to differentiate into various cell types. There is evidence that ES or iPS cells recapitulate normal developmental processes, and can serve as an alternative resource for hepatological researches, drug development and clinical uses. Through our present knowledge of developmental biology, efficient induction of hepatic lineage cells has been established. For example, based on the evidence that TGFβ–activin–Smad2 signaling is involved in definitive endoderm formation in the mouse (Tremblay et al., 2000), the activation of Activin–Nodal signaling was used for endoderm induction (D'Amour et al., 2005; Kubo et al., 2004). Fibroblast growth factor (FGF) and bone morphogenetic protein (BMP) were added for the specification of liver lineages (Jung, 1999; Mfopou et al., 2010; Shiraki et al., 2008a); this helped to mimic the mesodermal signals from the septum transversum mesenchyme in normal development (Katsumoto et al., 2010; Shin et al., 2007; Rossi et al., 2001). Because hepatocyte growth factors are known to be important effectors in the specification of cell fate and organogenesis of the liver (Schmidt et al., 1995; Sonnenberg et al., 1993), hepatocyte growth factor (HGF), dexamethasone and oncostatin M have been used for induction of hepatocyte maturation (Basma et al., 2009; Kamiya et al., 1999; Si-Tayeb et al., 2010). Compared with the factors described above that direct hepatic differentiation, the role of extracellular matrices (ECMs) and scaffolds remains unclear.

We have previously reported that culturing ES/iPS cells on the mesonephric M15 cell line, in the presence of specific growth factors, resulted in an efficient induction of endoderm-derived tissues, such as the liver or pancreas (Shiraki et al., 2008a; Shiraki et al., 2008b; Umeda et al., 2013). We further suggested that the basement membrane components, including *lama5*, play an important role in guiding the differentiation of ES cells into regional-specific lineages of the definitive endoderm (Higuchi et al., 2010). We also successfully established an alternative hepatic differentiation procedure without using feeder cells, but with a synthesized basement membrane (sBM) substratum (Higuchi et al., 2010; Shiraki et al., 2011). Together, these results revealed the importance of the ECM for differentiation of ES cells.

The basement membrane, a highly integrated three-dimensional structure composed of ECM molecules, is known to regulate various cellular processes. It is known that electrospun nanofibers provide not only three-dimensional microenvironments mimicking the ECM, but also appropriate guidance cues to modulate cell behavior. Here, we tested the effects of synthetic nanofiber (sNF) matrices on ES/iPS cell differentiation. We found that ES/iPS cells grown on the sNF were induced into endoderm and then hepatic fates. Overall, we conclude that the sNF is more potent in promoting hepatic differentiation, compared with the traditional two-dimensional culture surfaces, and is able to substitute for the sBM or M15 cells.

Results

Differentiation of murine and human ES cells into the hepatic lineages on the sNF matrix

We first tested the sNF matrix for its potency to mimic the basement membrane substratum of the cells. Murine SK7 ES cells (Shiraki et al., 2008a) were seeded onto the sNF matrix, and allowed to differentiate into the hepatic lineage by sequential changes of medium containing specific growth factors (Fig. 1A). We found that the expression of the pluripotent marker *Oct3/4* was downregulated, whereas the mesendoderm marker *Gsc* and definitive endoderm markers *Sox17* and *Foxa2* were expressed at day 4 (d4) of differentiation (Fig. 1B). Whereas *Gsc* was downregulated rapidly, *Sox17* and *Foxa2* showed peak expressions around d7 and were downregulated afterwards. Notably, the hepatic progenitor marker gene, alpha-fetoprotein (*Afp*), and the mature hepatocyte marker, albumin (*Alb1*) were detectable from d12 and d16, respectively, and their expression levels were increased with time. Although the *Afp* transcript level was decreased after d22, the *Alb1* expression continued increasing beyond d22. The immunocytochemical analysis further confirms that ALB and AFP were present in the cytoplasm of differentiated ES cells (Fig. 1C). In addition, periodic-acid–Schiff (PAS) staining and the Indocyanin Green (ICG) test were also conducted to investigate the hepatocyte functions of differentiated ES cells. The former reflects glycogen storage by showing positive populations as magenta in the cytoplasm, and the latter is used to examine cellular uptake activities, which are regarded as a hepatocyte detoxification function. As shown in Fig. 1D, glycogen storage was observed as the accumulation of magenta staining in the cytoplasm of the differentiated cells (top panel) and the ICG test also shows a similar result (bottom panel).

We next investigated whether human ES or iPS cells could differentiate in the sNF system. We used khES3 human ES cells

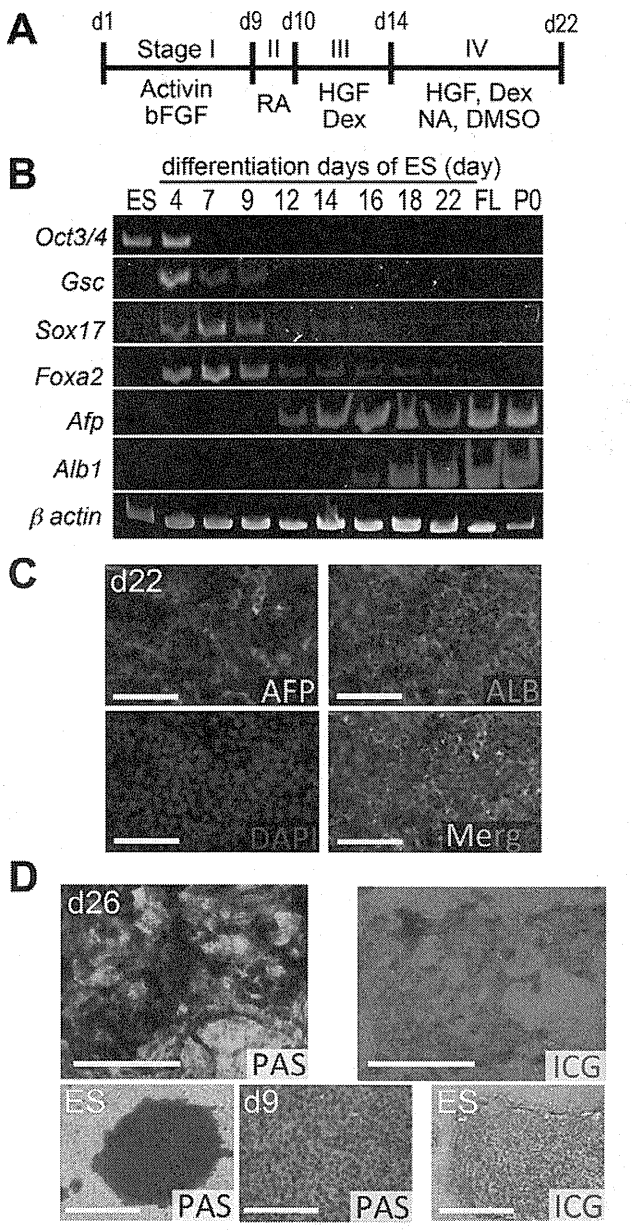

Fig. 1. Differentiation of murine ES cells into the hepatocyte lineage on nanofiber scaffolds. (A) Schematic diagram of the differentiation procedure for mouse ES cells. (B) Time-dependent expression levels of endoderm and hepatic marker genes. β-actin was used as a control. FL, fetal liver on embryonic day 12.5; P0, neonatal liver on postnatal day 0. (C) The immunochemical analysis of differentiated ES cells on day 22 (d22) for α-fetoprotein (AFP, green) and albumin (ALB, red) with nuclear counterstaining (DAPI). (D) Hepatocyte functional tests for PAS and ICG on d26 differentiated ES cells (top panels) and undifferentiated (bottom left and right panels) and d9 differentiated (bottom middle panel) ES cells as negative controls (bottom panels). Nuclei are counterstained with hematoxylin (blue). Scale bars: 250 μm.

(supplementary material Fig. S1A–D), as well as human iPS cell lines, such as Toe (supplementary material Fig. S1E,G) and 201B7 (supplementary material Fig. S1F), and found that these cells were able to differentiate into hepatocyte-like cells, thereby

producing ALB and taking up ICG (supplementary material Fig. S1D–G). Together, these results indicate that sNF is a suitable matrix for potentiating hepatic differentiation, not only in murine cells, but also in human ES cells and iPS cells.

sNF is more potent than normal plates precoated with other matrices

To compare the supportive effects of NFs and other substrata, we seeded murine ES cells onto either the sNF matrix or normal plates precoated with other stubstrata, including collagen I, Matrigel, gelatin and fibronectin and then performed the differentiation experiment as described in Fig. 1A. On differentiation day 22 (d22), quantitative PCR analyses were carried out to quantify the expression profiles of hepatic function marker genes in differentiated cells. Our results indicate that ES cells grown on sNF showed higher expression levels of proteins secreted by hepatocytes, such as serine peptidase inhibitor a1 (*Serpina1*), *Ttr* and *Alb1*, compared with those grown on other substrata (Fig. 2). Similar results were observed for the expression of several other genes, including glucose 6-phosphatase (*G6p*) and fatty-acid

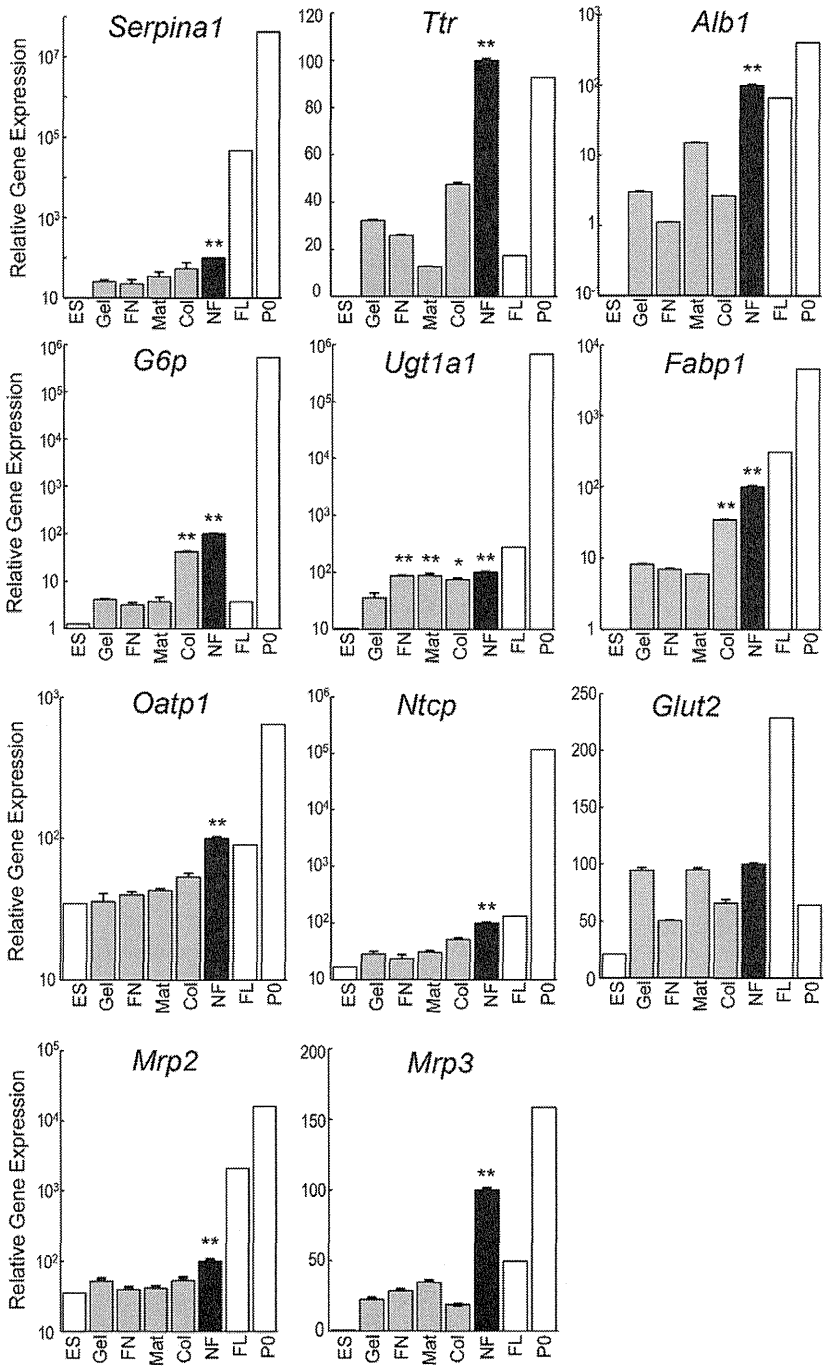

Fig. 2. Expression of hepatic markers in differentiated murine ES cells on sNF or other substrata. Expression levels of various gene transcripts quantified by real time PCR in d22 differentiated ES cells cultured on sNF, collagen I (Col), Matrigel (Mat), fibronectin (FN) or gelatin (Gel). ES, undifferentiated ES cells. FL (E12.5 fetal liver) and P0 (neonatal liver on postnatal day 0) are used as references. For differentiated ES cells, values represent mean ± s.e.m. (n=3). *P<0.05 and **P<0.01, by one-way ANOVA with the post-hoc Dunnett's test.

binding protein (*Fabp1*), or transporters, such as organic anion-transporting polypeptide 1 (*Oatp1*), Na^+-taurocholate cotransporting polypeptide (*Ntcp*) and UDP-glucuronosyltransferase (*Ugt1a1*), as well as multidrug resistance-associated protein family proteins 2 and 3 (*Mrp2* and *Mrp3*) (Fig. 2). By contrast, little change was found in the expression of glucose transporter 2 (*Glut2*).

To determine the hepatic functions of differentiated ES cells grown on Matrigel, collagen I or sNF, we next measured their ALB secretions, ICG uptake and cytochrome p450 (CYP) activities. Our results show that ES cells grown on sNF secreted ALB at a higher level compared with those on Matrigel or collagen I (Fig. 3A). By day 26, the percentage of ICG-positive ES cells on sNF was also higher than in ES cells grown on the other two substrates (Fig. 3B,C).

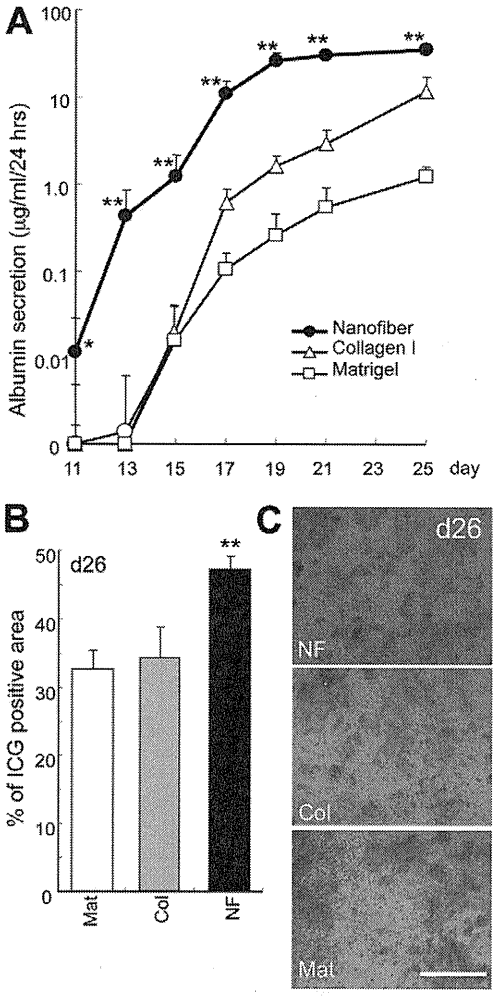

Fig. 3. Liver functional assays of differentiated murine ES cells grown on nanofiber scaffolds versus other substrata. (A) ELISA analysis of time-dependent albumin secretion for 24 hours by ES cells grown on Matrigel (Mat), collagen I (Col) or NF. (B,C) ICG tests performed on d26 differentiatied ES cells. The percentage of cells taking up ICG in culture was calculated (B) and representative images are shown (C). Values represent means ± s.e.m. (n=6). *P<0.05, **P<0.01, by two-tailed Student's t-test. Scale bar: 250 μm.

To measure CYP activities, the differentiated ES cells were treated with a CYP1A inducer, 3-methylcholantrene (3MC), for 48 hours during d22–d24 or d64–d66, as shown in supplementary material Fig. S2A. We found that the differentiated cells cultured on sNF had higher CYP1A1 activities and responses to the inducer than those cultured on fibronectin, Matrigel or collagen I (supplementary material Fig. S2B). We also assayed the effects of sNF on the maintenance of the mature hepatic cells. ES cells cultured on sNF were able to maintain their CYP1A1 activities and responses to 3MC even on d66, whereas those cultured on other matrices did not survive in long-term cultures (supplementary material Fig. S2C). It is also worth noting that the differentiated cells on sNF could be maintained in culture for more than 100 days. Specifically, we show that the ES cells cultured on sNF for 129 days were able to uptake and secrete ICG (supplementary material Fig. S2D). Based on these findings, we conclude that sNF is an excellent matrix, not only for the differentiation of ES cells into the hepatic lineage but also for maintaining the mature state of ES-cell-derived hepatocytes.

High Rac1 activities in undifferentiated and differentiated ES cells grown on sNF

Next, we investigated the effects of sNF on hepatic differentiation of ES cells. It was previously reported that the undifferentiated murine ES cells cultured on sNF exhibited spheroid morphologies and formed dome-like structures, and proliferated well (Nur-E-Kamal et al., 2006). Therefore, we checked the morphological changes between the undifferentiated and differentiated states of the murine ES cells. To exclude the effect of the extracellular matrix, we compared gelatin-coated normal two-dimensional (2D) plates with either gelatin-coated or uncoated sNF. We found that the undifferentiated ES cells grown on gelatin-coated 2D plates, with cytoplasmic spreading morphologies and attached to the plate surface in large areas (Fig. 4A, left). By contrast, the ES cells grown on sNF showed aggregated morphologies (Fig. 4A, middle and right).

In the differentiated state, the ES cells were found to form a monolayer on sNF. However, the morphological differences were still observed between ES cells cultured on sNF or normal 2D plates (Fig. 4B). Because these morphological changes are known to be regulated by cytoskeletal molecules, such as small Rho GTPase family member proteins, we next examined Rac1 activities in undifferentiated and differentiated ES cells. Our western blot analyses demonstrate that the GTP-bound active form of Rac1 was expressed at a higher level in ES cells cultured on sNF than those cultured on normal 2D plates, even though total Rac1 expression levels were similar (Fig. 4C,D). Interestingly, both the undifferentiated (Fig. 4C) and the differentiated ES cells on d8 (Fig. 4D) showed higher Rac-GTP activities. These results not only agree with the morphological differences of the ES cells, but also suggest that activated Rac1 plays a crucial role in potentiating the differentiation activity of ES cells cultured on sNF into hepatic lineages.

A crucial role of Rac activation in potentiating the differentiation of ES cells into the definitive endoderm and hepatocyte lineages

NSC23766 is a selective inhibitor of Rac1 activation that is mediated by the Rac-specific guanine nucleotide exchange factors (GEFs) TrioN and Tiam1, without affecting other Rho

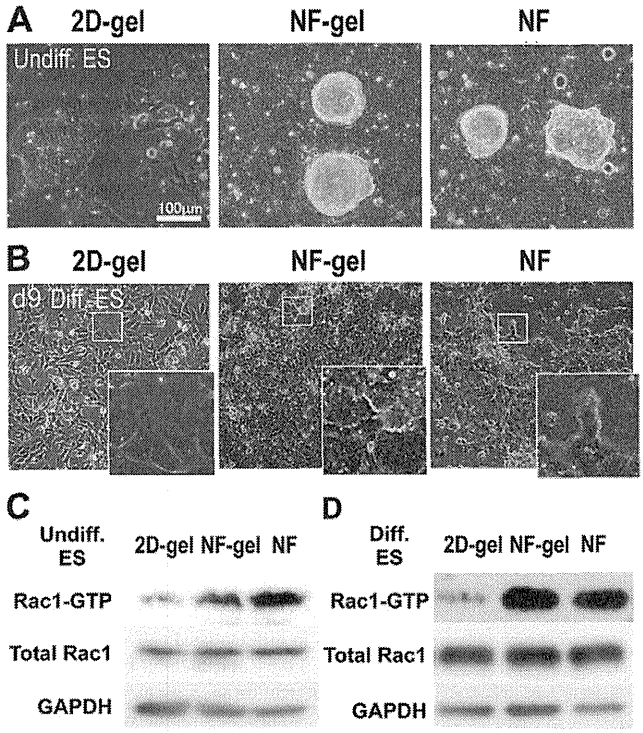

Fig. 4. NF induces Rac1 hydroxylation in both undifferentiated and day 9 differentiated murine ES cells. (A,B) Representative images of undifferentiated (A) and day 9 (d9) differentiated (B) ES cells grown on gelatin-precoated normal plates (2D-gel), gelatin-coated NF plates (NF-gel) and uncoated NF plates (NF). Insets are higher magnifications of the boxed regions. (C,D) Western blot analysis of GTP-bound active Rac1, total Rac1 and GAPDH expression in undifferentiated (C) or differentiated (D) ES cells described in A,B.

family members, such as RhoA or Cdc42 (Gao et al., 2004). We confirmed that 100 μM NSC23766 inhibited Rac1 hydroxylation (supplementary material Fig. 3A). To test whether sNF potentiates the differentiation of ES cells into the hepatic lineages through Rac1 activation, we treated murine ES cells with 100 μM NSC23766 at various stages and then determined the expression of stage-specific markers (Fig. 5A–C). We first added NSC23766 for 4 days at stage I to examine the effect of Rac1 activation on endoderm induction (Fig. 5A). We found that *Foxa2* expression was downregulated by the Rac1 inhibitor in ES cells cultured on sNF (Fig. 5A). We next examined the effects of Rac1 inhibition on hepatic differentiation. Our results show that the Rac1 inhibitor added at stage II (Fig. 5B) or stage III (Fig. 5C) downregulated the expression of hepatic markers, *Afp* or *Alb1*, on d10 or d14, respectively.

These results suggested that Rac1 activation is crucial for endoderm and hepatic differentiation. We subsequently examined the stage dependency of hepatic differentiation on Rac1 activities. The Rac1 inhibitor was added at different stages (I, II, III or IV) and *Alb1* expression was assayed on day 18 (Fig. 5D). We found that Rac1 inhibition at all four stages blocked the potentiating effects of sNF, and resulted in decreases in *Alb1* expression. These results further confirm the important role of Rac1 and demonstrate that continuous activation of Rac1 is crucial for the potentiation of hepatic differentiation.

Then we confirmed whether NSC23766 had any effect on the proliferation of ES cells. NSC23766 decreased the proportion of EdU-positive cells in stages I, II and III, particularly in stage I, without apparent toxicity (supplementary material Fig. S3C). Interestingly, the total numbers of cells in the NSC23766-treated groups was smaller in stages I and II, which became greater than that of control groups used in stages III and IV (supplementary material Fig. S3B). Taken together, these findings suggest that Rac1 differentially contributes to proliferation in the early differentiation stages and promotes differentiation in the late stage.

Discussion

Our previous study suggested that although addition of soluble growth factors is sufficient to promote the differentiation of ES cells into the definitive endoderm, further differentiation from the definitive endoderm into hepatic and pancreatic fates appears to require a direct contact with M15 cells (Shiraki et al., 2008a). We previously showed the importance of basement membrane substratum by culturing ES cells on sBM (Higuchi et al., 2010; Shiraki et al., 2011). Specifically, ES cells grown on sBM were able to differentiate into hepatic and pancreatic lineages. These results imply that the basement membrane structure plays a major role in the differentiation of ES cells. Although the sBM used previously was constructed by overexpressing recombinant laminin-511 (laminin α5, laminin β1 and laminin γ1) in H293 cells (Doi et al., 2002), ES cells or iPS cells could be induced into the hepatic and pancreatic lineages. The efficacy of such an sBM for differentiation was high, and the differentiated cells could perform liver-specific functions, such as protein secretion, detoxification and glycogen storage (Higuchi et al., 2010; Shiraki et al., 2011).

The nanofiber produced by the electrospinning technique is a chemically and physically stable synthetic three-dimensional surface that mimics the structural geometry and porosity of the basement membrane or ECM (Schindler et al., 2005; Schindler et al., 2006). NF scaffolds have been shown to recapitulate the structural features of stem cell niche (Lim and Mao, 2009) and have been used for the *ex vivo* expansion of various types of stem cells such as murine ES cells (Hashemi et al., 2011; Nur-E-Kamal et al., 2006) and human tissue stem cells. In addition, the ECM was found to deposit as an extensive scaffold on the basal surface of the cells attached to NFs (Shih et al., 2006; Chua et al., 2007; Ma et al., 2008). Importantly, the sNF system has been reported to enhance not only the differentiation of murine ES cells into neural lineages (Lim et al., 2010; Purcell et al., 2012; Xie et al., 2009), but also differentiation from human MSCs into hepatoblasts (Ghaedi et al., 2012; Kazemnejad et al., 2009).

Taken together, these previous observations revealed that the sNF matrix is useful as a substratum to replace feeder cells and that it has the ability to potentiate hepatic differentiation. In this study, we show that both murine and human ES cells, as well as human iPS cells, could differentiate on sNF and exhibit liver-specific functions. Furthermore, we demonstrate that Rac1 activation was involved in hepatic differentiation. Rac1, a member of the Rho family GTP-binding proteins, including Rho and Cdc42 (Heasman and Ridley, 2008), functions by activating actin-rich lamellipodial protrusion and membrane ruffling, which are thought to be a major part of the driving force for cell movement (Nobes and Hall, 1995; Ridley et al., 1992). Although Rho family proteins were reported to be

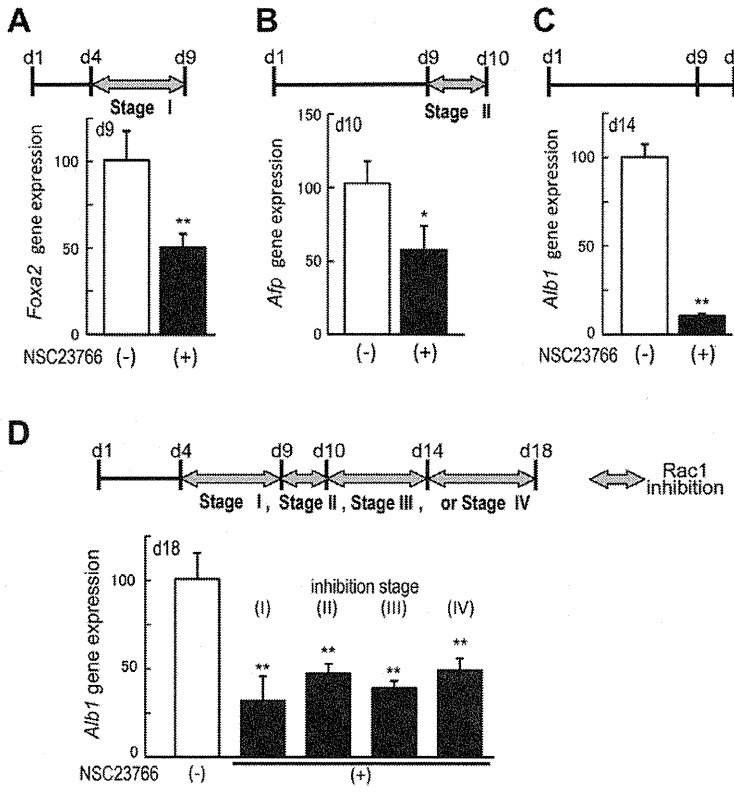

Fig. 5. Inhibition of the Rac1 pathway blocks the differentiation-potentiating activity of NF. (A–C) Quantitative PCR analysis of the gene expression of *Foxa2* (A), *Afp* (B) and *Alb1* (C), in differentiated cells cultured on sNF with (+) or without (−) the Rac1 inhibitor NSC23766 (100 μM), at the end of stage I (A), stage II (B) or stage III (C). (D) The expression of *Alb1* on day 18 in differentiated cells, treated with (+) or without (−) the Rac1 inhibitor at indicated stages. Data shown represent mean ± s.e.m. ($n=3$); $^{*}P<0.05$ and $^{**}P<0.01$, compared with untreated cells on sNF with the Rac1 inhibitor by two-tailed Student's *t*-test or one-way ANOVA with the post-hoc Dunnett's test.

expressed by ES cells cultured on sNF (Nur-E-Kamal et al., 2005; Nur-E-Kamal et al., 2006; Schindler et al., 2006), their roles have never been investigated.

In vivo developmental processes occurring in the endoderm and its derivatives cause dynamic migration during gastrulation and later stages of organogenesis (Woo et al., 2012), suggesting that motility and differentiation are closely inter-related. In this study, we observed that ES cells cultured on sNF showed greater Rac1 activation than did cells cultured on the normal 2D surface. Indeed, Rac1 is known to be involved in not only endoderm induction but also hepatic specification and maturation. In particular, *Rac1* mutant mice died by mouse embryonic day 9.5 (E9.5) because of severe developmental abnormalities, and *Rac1*-deficient embryos showed numerous cell deaths in the space between the ectoderm and endoderm at the primitive streak stage (Sugihara et al., 1998). Rac1 is also important for cellular differentiation, for example, epithelial differentiation in the small intestine (Stappenbeck and Gordon, 2000), pancreatic islet morphogenesis (Greiner et al., 2009), myogenic differentiation (Heller et al., 2001), maintenance of the thymic epithelial cells (Hunziker et al., 2011), formation of the lens (Maddala et al., 2011) and neuronal development (Corbetta et al., 2009; Leone et al., 2010). In addition, Rac1 has been shown to crosstalk with many downstream signaling pathways such as Wnt (Clarke, 2006; Malliri et al., 2006), TGF-β1 (Varon et al., 2008), Nodal (Woo et al., 2012), retinoic acid (Lee et al., 2008) and Myc (Hunziker et al., 2011; Nikolova et al., 2008). Interestingly, Rac1 is also known to mediate stem cell-shape-dependent regulation of differentiation to a chondrogenic versus myogenic fate (Gao et al., 2010). On the basis of these studies, we postulate that the sNF system might potentiate ES cells to differentiate into hepatic lineages by interacting downstream of certain growth factors during differentiation processes.

In conclusion, we show that Rac1 was activated in both undifferentiated and differentiated ES cells cultured on sNF plates and that Rac1 inhibition blocked the potentiating effects of sNF on endoderm and hepatic differentiation. These results suggest that continuous activation of Rac1 throughout the differentiation stage is crucial for potentiating differentiation. Our results also highlight the morphological changes during differentiation along the Rac1 pathway, which controls cellular morphology, motility and differentiation into the hepatic lineage. Here, we established a completely chemically defined method that requires no serum or no xenogenic substrata, thereby eliminating the risk of contamination with unknown factors. We believe that this novel method could be an attractive culture model for pharmacological research and research on stem cell biology and therapeutic strategies.

Materials and Methods

ES and iPS cell lines

The murine ES cell line, SK7 (Shiraki et al., 2008a) was maintained on mouse embryonic fibroblast (MEF) feeders in Glasgow minimum essential medium (Invitrogen, Glasgow, UK) supplemented with 1000 units/ml leukemia inhibitory factor (LIF; Chemicon, Temecula, CA), 15% knocked-out serum replacement (KSR; Invitrogen), 1% fetal bovine serum (FBS; Hyclone, Logan, UT), 100 μM nonessential amino acids (NEAA; Invitrogen), 2 mM L-glutamine (L-Gln; Invitrogen), 1 mM sodium pyruvate (Invitrogen), 50 units/ml penicillin and 50 μg/ml streptomycin (PS; Invitrogen) and 100 μM β-mercaptoethanol (β-ME; Sigma-Aldrich, St Louis, MO).

Human ES cells (KhES-3) (Suemori et al., 2006) were from Dr Norio Nakatsuji and Dr Hirofumi Suemori (Kyoto University, Kyoto, Japan). They were used in accordance with the human ES cell guidelines of the Japanese government. This human ES work was approved by Kumamoto University institutional review board. Human iPS 201B7 cells were a gift from Dr Yamanaka (Kyoto University, Kyoto, Japan). The human iPS Toe cell line was established by M. Toyoda and

colleagues (National Institute for Child Health and Development, Tokyo, Japan). Undifferentiated human ES and iPS cells were maintained as described previously (Shiraki et al., 2008b).

Culture plates

Synthetic nanofiber (sNF) matrices were purchased from Corning Coster (Ultra-Web Synthetic Polyamine Surface #3873XX1; Cambridge, MA). Plate surfaces were coated with electrospun polyamide nanofibers. sNF matrices consisted of two kinds of polyamide polymers, A $(C_{28}O_4N_4H_{47})_n$ and B $(C_{28}O_{4.4}N_4H_{47})_n$, which were crosslinked in the presence of an acid catalyst, and were 200–400 nm in diameter (average 280 nm). Pore sizes, similar to those of the cell basement membrane, were ~700 nm. For comparison, Corning 96-well plates were pretreated for 3 hours at 37℃ with 0.1% gelatin (Sigma-Aldrich), Matrigel (BD, Franklin Lakes, NJ) or CellStart (Invitrogen). Collagen I (Nitta Gelatin, Japan) was diluted with Dulbecco's modified Eagle's medium (DMEM; Invitrogen) at a concentration of 1 mg/ml and plate surfaces were treated for 15 minutes, then dried until use.

Differentiation of murine ES cells into hepatic lineages on sNF

Murine ES cells plated at a density of 1.5×10^4 cells/cm^2 in culture plates described above were grown for 8 days in DMEM containing 4,500 mg/l glucose, s NEAA, L-Gln, PS, β-ME, 10 mg/ml insulin, 5.5 mg/ml transferrin, 6.7 pg/ml selenium (Insulin-Transferrin-Selenium-G Supplement; ITS, Invitrogen), 0.25% AlbuMAX II (Invitrogen), 10 ng/ml recombinant human activin-A (R&D Systems, Minneapolis, MN), 5 ng/ml; recombinant human bFGF, and cultured for 8 days. On day 9 (d9), the medium was changed to RPMI-1640 (Invitrogen) containing 10^{-6} M retinoic acid (RA; Stemolecule all-trans retinoic acid; Stemgent, Cambridge, MA) and B27 supplement (Invitrogen). On d10, medium was switched to 2000 mg/l glucose DMEM (Invitrogen), 10% KSR, 10 ng/ml recombinant human hepatocyte growth factor (Peprotech, Rocky Hill, NJ) and 10 μM dexamethasone (Sigma-Aldrich), and cultured until d14. Next, 1 mM nicotinamide (NA; Sigma-Aldrich) and 1% dimethylsufoxide (DMSO; Sigma-Aldrich), were added to medium and KSR was removed. Medium was replaced every 2 days with fresh medium and growth factors.

Human ES/iPS cells were pretreated with the ROCK inhibitor Y27632 (Wako, Japan) 1 day before trypsinization. Cells were plated at a density of 3×10^5 cells/cm^2 on Matrigel-coated sNF matrices with Y27632. The following two procedures were subsequently used to induce hepatic differentiation of various human ES/iPS cells; simplified (two-step) protocol, KhES3 and 201B7 cells; or conventional (three-step) protocol, Toe cells. In the simplified protocol, medium used at first contained B27 and 100 ng/ml activin-A in RPMI-1640, which was then, switched to 10 ng/ml HGF, 10 μM dexamethasone, 0.5% DMSO, 0.5 mM NA. In the conventional protocol, medium used first was the same as that in the simplified protocol, followed by 1% DMSO and 20% KSR in knockout DMEM/F12 (Invitrogen) for 6 days and, then DMEM containing HGF, dexamethasone and 10% KSR. Finally, the above medium was added with 0.5 mM NA. Medium was replaced every 2 days with fresh medium and growth factors. KhES3 and 201B7 cells were induced hepatic differentiation with simplified protocol, and Toe cells were treated with conventional protocol.

Periodic-acid–Schiff's staining

For detection of glycogen storage in the differentiated cells, periodic-acid–Schiff's (PAS) staining kit (Muto Pure Chemicals, Tokyo, Japan) was used. Cells cultured for 9 and 26 days, and undifferentiated ES cells were fixed in 3.3% formalin for 10 minutes, and stained following the manufacturer's instructions, then nuclear counterstaining with hematoxylin (blue) was performed.

Albumin secretion assay

The culture medium was replaced with fresh medium every 2 days, and supernatants were collected 24 hours after replacing the medium. The mouse (human) albumin secreted in the supernatant was determined using a mouse (human) ELISA quantification kit (Bethyl, Montgomery, TX).

Indocyanine Green (ICG) test

Indocyanine Green (Daiichi-Sankyo Pharm., Japan) was diluted with the above culture medium to a final concentration of 1 mg/dl. The ICG test solution was added to the differentiated ES cells after the appropriate culture periods and undifferentiated ES cells were used as controls, and incubated at 37℃ for 30 minutes. Then, after three washes with phosphate-buffered saline (PBS), the cellular uptake of ICG was examined by microscopy. The percentage ICG-positive areas represent the proportion of ICG-positive area versus total cell area, which were determined using ImageJ software (US National Institutes of Health, Bethesda, MD).

CYP inductions

To check the inducibilities of cytochrome P450 activities in response to inducers, we used the P450-Glo CYP Assay Kit (Promega, Madison, WI). The differentiated ES cells were treated with 5 μM 3-methylcholantrene as inducers of CYP1A. The medium containing the inducers was changed every 24 hours. 48 hours after treatment, we changed the medium and used the appropriate luminogenic CYP substrates (Luciferine-CEE for CYP1A). The cells were incubated at 37℃ for 3 hours, and then the supernatants were mixed with equal amount of detection reagent, according to the manufacturer's instructions. The luminescence was measured using a GloMax 96 microplate luminometer (Promega), and luminometer settings were as in the manufacturer's instructions. Cell numbers were calculated using CellTiter-Glo luminescent cell viability assays (Promega) to normalize P450-Glo assay values to cell number.

Immunocytochemistry

After culture for the appropriate times, cells were fixed in 4% paraformaldehyde in PBS for 30 minutes at room temperature. After removal of paraformaldehyde solution, the fixed cells were permeabilized with 0.1% Triton X-100 for 10 minutes. The permeabilized cells were rinsed several times with PBS and were then incubated with 20% Blocking One (Nacalai Tesque, Japan) in PBST (0.1% Tween-20 in PBS) for blocking. After blocking, the cells were incubated with the diluted antibody in 20% Blocking One in PBST (0.1% Tween-20 in PBS) in a humidified chamber overnight at 4℃. After washing the cells in PBST, cells were incubated with the secondary antibody in 20% Blocking One for 2 hours at room temperature in the dark. After washing off the secondary antibody in PBST, cells were counterstained with 6-diamidino-2-phenylindole (DAPI) (Roche Diagnostics, Switzerland). The following antibodies were used as primary antibodies: rabbit anti-alphafeto protein (Dako, Denmark), goat anti-albumin (Sigma-Aldrich), goat anti-Sox17, mouse anti-FoxA2 (R&D systems); secondary antibodies used were conjugated to Alexa Fluor 568, Alexa Fluor 488 and Alexa Fluor 633 (Invitrogen). For human ES cell cultures, goat antibodies against human albumin (Bethyl) were used as primary antibodies.

Cell proliferation assay

Cell proliferation was evaluated using Click-iT EdU assay kit (invitrogen). The cells cultured with or without NSC23766 were exposed to 10 μM of 5-ethnyl-2′-deoxyuridine (EdU) for 1 hour at 37℃ before fixation. The fixed cells were processed for immunocytochemistry as described above, with an additional step for EdU detection. Before incubation with secondary antibodies, the cells were incubated with EdU in the Click-iT reaction cocktail and Alexa Fluor 488 for 30 minutes at room temperature, following the manufacturer's instructions. Images were collected using ImageXpress Micro (Molecular Devices) and EdU-positive nuclei per total number of nuclei were counted.

RT-PCR analysis

RNA was extracted from ES cells or mouse liver using an RNeasy mini-kit (Qiagen, Germany) and then treated with DNase (Qiagen). For reverse transcription reactions, 3 μg RNA was reverse-transcribed using ReverTra Ace (Toyobo, Japan) and oligo dT primers (Toyobo). One μl of fivefold-diluted cDNA (1% of the RT product) was used for PCR analyses. The primer sequences for each primer set are shown in supplementary material Table S1. For real-time PCR analysis, mRNA expression was quantified with SyberGreen on an ABI 7500 thermal cycler (Applied Biosystems, Foster City, CA). The PCR conditions were as follows: denaturation at 95℃ for 15 seconds, annealing and extention at 60℃ for 60 seconds, for up to 40 cycles. Each measurement was normalized to β-actin (mouse) and *GAPDH* (human) for each sample by subtracting the average β-actin (mouse) and *GAPDH* (human) C_t values (Threshold Cycle) from the average C_t for each gene. Target mRNA levels, expressed as arbitrary units, were determined using a standard curve method.

Rac pull-down assay

Murine ES cells were trypsinized and suspended at a density of 5×10^4 cells/ml. Cells were then plated onto sNF either with or without 0.1% gelatin pretreatment; control plates were pretreated with 0.1% gelatin. Undifferentiated cells were harvested 48 hours after incubation under ES cell maintenance culture conditions at 37℃, whereas differentiated cells were harvested 9 days after hepatic differentiation started. The activation of Rac was determined using a Rac1 Activation Assay Kit purchased from Millipore. Briefly, cells were washed with PBS and suspended in lysis buffer provided by the supplier. Aliquots were taken from each cell lysate, and the amount of GAPDH proteins present in the lysates was determined and used for normalization. GTP-bound forms of Rac were then pulled down from lysates using reagents provided by the supplier, following the recommended instructions. Proteins present in total cell lysates or Rac pull-down samples were separated by SDS-PAGE (12%) and transferred onto a nylon membrane. Western blotting was performed using antibodies against Rac1, according to the ECL protocol provided by the suppliers. Luminescence of Rac1 bands was quantified using the GE ImageQuant LAS 4000 (GE Healthcare Life Science, Sweden).

Acknowledgements

We thank members of Gene Technology Center in Kumamoto University for their technical assistance.

Author contributions

T.Y. performed cellular and biochemical analyses; T.Y. and N.S. established the ES cell differentiation system; M.T., N.K., H.O., Y.M., H.A. and A.U. established human iPS Toe cell line; Y.S., K.K. and S.K. provided technical advice, designed the experiments and wrote the paper. All authors discussed the results and commented on the manuscript.

Funding

This work was supported by a grant (to S.K.) from the Realization of Regenerative Medicine from the Ministry of Education, Culture, Sports, Science and Technology (MEXT) Japan; a grant from National Institute of Biomedical Innovation (to N.S.); a funding program for Next Generation World-Leading Researchers (NEXT Program) from the Japan Society for the Promotion of Science (JSPS) [grant number LS099 to S.K.] (to S.K.); and the Program for Leading Graduate Schools "HIGO" (to S.K.) a global COE grant (Cell Fate Regulation Research and Education Unit) from MEXT. S.K. was a member of Program (Cell Fate Regulation Research and Education Unit), MEXT, Japan.

Supplementary material available online at
http://jcs.biologists.org/lookup/suppl/doi:10.1242/jcs.129767/-/DC1

References

Basma, H., Soto-Gutiérrez, A., Yannam, G. R., Liu, L., Ito, R., Yamamoto, T., Ellis, E., Carson, S. D., Sato, S., Chen, Y. et al. (2009). Differentiation and transplantation of human embryonic stem cell-derived hepatocytes. *Gastroenterology* **136**, 990-999.

Chua, K.-N., Chai, C., Lee, P.-C., Ramakrishna, S., Leong, K. W. and Mao, H.-Q. (2007). Functional nanofiber scaffolds with different spacers modulate adhesion and expansion of cryopreserved umbilical cord blood hematopoietic stem/progenitor cells. *Exp. Hematol.* **35**, 771-781.

Clarke, R. (2006). Wnt signalling in the mouse intestine. *Oncogene* **25**, 7512-7521.

Corbetta, S., Gualdoni, S., Ciceri, G., Monari, M., Zuccaro, E., Tybulewicz, V. L. J. and de Curtis, I. (2009). Essential role of Rac1 and Rac3 GTPases in neuronal development. *FASEB J.* **23**, 1347-1357.

D'Amour, K. A., Agulnick, A. D., Eliazer, S., Kelly, O. G., Kroon, E. and Baetge, E. E. (2005). Efficient differentiation of human embryonic stem cells to definitive endoderm. *Nat. Biotechnol.* **23**, 1534-1541.

Doi, M., Thyboll, J., Kortesmaa, J., Jansson, K., Iivanainen, A., Parvardeh, M., Timpl, R., Hedin, U., Swedenborg, J. and Tryggvason, K. (2002). Recombinant human laminin-10 (alpha5beta1gamma1). Production, purification, and migration-promoting activity on vascular endothelial cells. *J. Biol. Chem.* **277**, 12741-12748.

Gao, Y., Dickerson, J. B., Guo, F., Zheng, J. and Zheng, Y. (2004). Rational design and characterization of a Rac GTPase-specific small molecule inhibitor. *Proc. Natl. Acad. Sci. USA* **101**, 7618-7623.

Gao, L., McBeath, R. and Chen, C. S. (2010). Stem cell shape regulates a chondrogenic versus myogenic fate through Rac1 and N-cadherin. *Stem Cells* **28**, 564-572.

Ghaedi, M., Soleimani, M., Shabani, I., Duan, Y. and Lotfi, A. S. (2012). Hepatic differentiation from human mesenchymal stem cells on a novel nanofiber scaffold. *Cell. Mol. Biol. Lett.* **17**, 89-106.

Greiner, T. U., Kesavan, G., Ståhlberg, A. and Semb, H. (2009). Rac1 regulates pancreatic islet morphogenesis. *BMC Dev. Biol.* **9**, 2.

Hashemi, S. M., Soudi, S., Shabani, I., Naderi, M. and Soleimani, M. (2011). The promotion of stemness and pluripotency following feeder-free culture of embryonic stem cells on collagen-grafted 3-dimensional nanofibrous scaffold. *Biomaterials* **32**, 7363-7374.

Heasman, S. J. and Ridley, A. J. (2008). Mammalian Rho GTPases: new insights into their functions from in vivo studies. *Nat. Rev. Mol. Cell Biol.* **9**, 690-701.

Heller, H., Gredinger, E. and Bengal, E. (2001). Rac1 inhibits myogenic differentiation by preventing the complete withdrawal of myoblasts from the cell cycle. *J. Biol. Chem.* **276**, 37307-37316.

Higuchi, Y., Shiraki, N., Yamane, K., Qin, Z., Mochitate, K., Araki, K., Senokuchi, T., Yamagata, K., Hara, M., Kume, K. et al. (2010). Synthesized basement membranes direct the differentiation of mouse embryonic stem cells into pancreatic lineages. *J. Cell Sci.* **123**, 2733-2742.

Hunziker, L., Benitah, S. A., Braun, K. M., Jensen, K., McNulty, K., Butler, C., Potton, E., Nye, E., Boyd, R., Laurent, G. et al. (2011). Rac1 deletion causes thymic atrophy. *PLoS ONE* **6**, e19292.

Jung, J. (1999). Initiation of mammalian liver development from endoderm by fibroblast growth factors. *Science* **284**, 1998-2003.

Kamiya, A., Kinoshita, T., Ito, Y., Matsui, T., Morikawa, Y., Senba, E., Nakashima, K., Taga, T., Yoshida, K., Kishimoto, T., et al. (1999). Fetal liver development requires a paracrine action of oncostatin M through the gp130 signal transducer. *EMBO J.* **18**, 2127-2136.

Katsumoto, K., Shiraki, N., Miki, R. and Kume, S. (2010). Embryonic and adult stem cell systems in mammals: ontology and regulation. *Dev. Growth Differ.* **52**, 115-129.

Kazemnejad, S., Allameh, A., Soleimani, M., Gharehbaghian, A., Mohammadi, Y., Amirizadeh, N. and Jazayery, M. (2009). Biochemical and molecular characterization of hepatocyte-like cells derived from human bone marrow mesenchymal stem cells on a novel three-dimensional biocompatible nanofibrous scaffold. *J. Gastroenterol. Hepatol.* **24**, 278-287.

Kubo, A., Shinozaki, K., Shannon, J. M., Kouskoff, V., Kennedy, M., Woo, S., Fehling, H. J. and Keller, G. (2004). Development of definitive endoderm from embryonic stem cells in culture. *Development* **131**, 1651-1662.

Lee, Y. M., Lee, J. O., Jung, J.-H., Kim, J. H., Park, S.-H., Park, J. M., Kim, E.-K., Suh, P.-G. and Kim, H. S. (2008). Retinoic acid leads to cytoskeletal rearrangement through AMPK-Rac1 and stimulates glucose uptake through AMPK-p38 MAPK in skeletal muscle cells. *J. Biol. Chem.* **283**, 33969-33974.

Leone, D. P., Srinivasan, K., Brakebusch, C. and McConnell, S. K. (2010). The rho GTPase Rac1 is required for proliferation and survival of progenitors in the developing forebrain. *Dev. Neurobiol.* **70**, 659-678.

Lim, S. H. and Mao, H.-Q. (2009). Electrospun scaffolds for stem cell engineering. *Adv. Drug Deliv. Rev.* **61**, 1084-1096.

Lim, S. H., Liu, X. Y., Song, H., Yarema, K. J. and Mao, H.-Q. (2010). The effect of nanofiber-guided cell alignment on the preferential differentiation of neural stem cells. *Biomaterials* **31**, 9031-9039.

Ma, K., Chan, C. K., Liao, S., Hwang, W. Y. K., Feng, Q. and Ramakrishna, S. (2008). Electrospun nanofiber scaffolds for rapid and rich capture of bone marrow-derived hematopoietic stem cells. *Biomaterials* **29**, 2096-2103.

Maddala, R., Chauhan, B. K., Walker, C., Zheng, Y., Robinson, M. L., Lang, R. A. and Rao, P. V. (2011). Rac1 GTPase-deficient mouse lens exhibits defects in shape, suture formation, fiber cell migration and survival. *Dev. Biol.* **360**, 30-43.

Malliri, A., Rygiel, T. P., van der Kammen, R. A., Song, J. Y., Engers, R., Hurlstone, A. F., Clevers, H. and Collard, J. G. (2006). The rac activator Tiam1 is a Wnt-responsive gene that modifies intestinal tumor development. *J. Biol. Chem.* **281**, 543-548.

Mfopou, J. K., Chen, B., Mateizel, I., Sermon, K. and Bouwens, L. (2010). Noggin, retinoids, and fibroblast growth factor regulate hepatic or pancreatic fate of human embryonic stem cells. *Gastroenterology* **138**, 2233–2245, 2245.e1-14.

Nikolova, E., Mitev, V., Minner, F., Deroanne, C. F. and Poumay, Y. (2008). The inhibition of the expression of the small Rho GTPase Rac1 induces differentiation with no effect on cell proliferation in growing human adult keratinocytes. *J. Cell. Biochem.* **103**, 857-864.

Nobes, C. D. and Hall, A. (1995). Rho, rac, and cdc42 GTPases regulate the assembly of multimolecular focal complexes associated with actin stress fibers, lamellipodia, and filopodia. *Cell* **81**, 53-62.

Nur-E-Kamal, A., Ahmed, I., Kamal, J., Schindler, M. and Meiners, S. (2005). Three dimensional nanofibrillar surfaces induce activation of Rac. *Biochem. Biophys. Res. Commun.* **331**, 428-434.

Nur-E-Kamal, A., Ahmed, I., Kamal, J., Schindler, M. and Meiners, S. (2006). Three-dimensional nanofibrillar surfaces promote self-renewal in mouse embryonic stem cells. *Stem Cells* **24**, 426-433.

Purcell, E. K., Naim, Y., Yang, A., Leach, M. K., Velkey, J. M., Duncan, R. K. and Corey, J. M. (2012). Combining topographical and genetic cues to promote neuronal fate specification in stem cells. *Biomacromolecules* **13**, 3427-3438.

Ridley, J., Paterson, H. F., Johnston, C. L., Diekmann, D. and Hall, A. (1992). The small GTP-binding protein rac regulates growth factor-induced membrane ruffling. *Cell* **70**, 401-410.

Rossi, J. M., Dunn, N. R., Hogan, B. L. and Zaret, K. S. (2001). Distinct mesodermal signals, including BMPs from the septum transversum mesenchyme, are required in combination for hepatogenesis from the endoderm. *Genes Dev.* **15**, 1998-2009.

Schindler, M., Nur-E-Kamal, A. and Ahmed, I. (2006). Living in three dimensions. *Cell Biochem.* **45**, 215-227.

Schindler, M., Ahmed, I., Kamal, J., Nur-E-Kamal, A., Grafe, T. H., Young Chung, H. and Meiners, S. (2005). A synthetic nanofibrillar matrix promotes in vivo-like organization and morphogenesis for cells in culture. *Biomaterials* **26**, 5624-5631.

Schmidt, C., Bladt, F., Goedecke, S., Brinkmann, V., Zschiesche, W., Sharpe, M., Gherardi, E. and Birchmeier, C. (1995). Scatter factor/hepatocyte growth factor is essential for liver development. *Nature* **373**, 699-702.

Shih, Y.-R. V., Chen, C.-N., Tsai, S.-W., Wang, Y. J. and Lee, O. K. (2006). Growth of mesenchymal stem cells on electrospun type I collagen nanofibers. *Stem Cells* **24**, 2391-2397.

Shin, D., Shin, C. H., Tucker, J., Ober, E. A., Rentzsch, F., Poss, K. D., Hammerschmidt, M., Mullins, M. C. and Stainier, D. Y. (2007). Bmp and Fgf signaling are essential for liver specification in zebrafish. *Development* **134**, 2041-2050.

Shiraki, N., Yoshida, T., Araki, K., Umezawa, A., Higuchi, Y., Goto, H., Kume, K. and Kume, S. (2008a). Guided differentiation of embryonic stem cells into Pdx1-expressing regional-specific definitive endoderm. *Stem Cells* **26**, 874-885.

Shiraki, N., Umeda, K., Sakashita, N., Takeya, M., Kume, K. and Kume, S. (2008b). Differentiation of mouse and human embryonic stem cells into hepatic lineages. *Genes Cells* **13**, 731-746.

Shiraki, N., Yamazoe, T., Qin, Z., Ohgomori, K., Mochitate, K., Kume, K. and Kume, S. (2011). Efficient differentiation of embryonic stem cells into hepatic cells in vitro using a feeder-free basement membrane substratum. *PLoS ONE* **6**, e24228.

Si-Tayeb, K., Noto, F. K., Nagaoka, M., Li, J., Battle, M. A., Duris, C., North, P. E., Dalton, S. and Duncan, S. A. (2010). Highly efficient generation of human hepatocyte-like cells from induced pluripotent stem cells. *Hepatology* **51**, 297-305.

Sonnenberg, E., Meyer, D., Weidner, K. M. and Birchmeier, C. (1993). Scatter factor/hepatocyte growth factor and its receptor, the c-met tyrosine kinase, can mediate a signal exchange between mesenchyme and epithelia during mouse development. *J. Cell Biol.* **123**, 223-235.

Stappenbeck, T. S. and Gordon, J. I. (2000). Rac1 mutations produce aberrant epithelial differentiation in the developing and adult mouse small intestine. *Development* **127**, 2629-2642.

Suemori, H., Yasuchika, K., Hasegawa, K., Fujioka, T., Tsuneyoshi, N. and Nakatsuji, N. (2006). Efficient establishment of human embryonic stem cell lines and long-term maintenance with stable karyotype by enzymatic bulk passage. *Biochem. Biophys. Res. Commun.* **345**, 926-932.

Sugihara, K., Nakatsuji, N., Nakamura, K., Nakao, K., Hashimoto, R., Otani, H., Sakagami, H., Kondo, H., Nozawa, S., Aiba, A. et al. (1998). Rac1 is required for the formation of three germ layers during gastrulation. *Oncogene* **17**, 3427-3433.

Tremblay, K. D., Hoodless, P. A., Bikoff, E. K. and Robertson, E. J. (2000). Formation of the definitive endoderm in mouse is a Smad2-dependent process. *Development* **127**, 3079-3090.

Umeda, K., Suzuki, K., Yamazoe, T., Shiraki, N., Higuchi, Y., Tokieda, K., Kume, K., Mitani, K. and Kume, S. (2013). Albumin gene targeting in human embryonic stem cells and induced pluripotent stem cells with helper-dependent adenoviral vector to monitor hepatic differentiation. *Stem Cell Res.* **10**, 179-194.

Varon, C., Rottiers, P., Ezan, J., Reuzeau, E., Basoni, C., Kramer, I. and Génot, E. (2008). TGFbeta1 regulates endothelial cell spreading and hypertrophy through a Rac-p38-mediated pathway. *Biol. Cell* **100**, 537-550.

Woo, S., Housley, M. P., Weiner, O. D. and Stainier, D. Y. R. (2012). Nodal signaling regulates endodermal cell motility and actin dynamics via Rac1 and Prex1. *J. Cell Biol.* **198**, 941-952.

Xie, J., Willerth, S. M., Li, X., Macewan, M. R., Rader, A., Sakiyama-Elbert, S. E. and Xia, Y. (2009). The differentiation of embryonic stem cells seeded on electrospun nanofibers into neural lineages. *Biomaterials* **30**, 354-362.

Journal of Cell Science

The Transcriptional Cofactor MCAF1/ATF7IP Is Involved in Histone Gene Expression and Cellular Senescence

Nobuhiro Sasai[1], Noriko Saitoh[1], Hisato Saitoh[2], Mitsuyoshi Nakao[1,3*]

1 Department of Medical Cell Biology, Institute of Molecular Embryology and Genetics, Kumamoto University, Kumamoto, Japan, **2** Department of Biological Sciences, Graduate School of Science and Technology, Kumamoto University, Kumamoto, Japan, **3** Core Research for Evolutional Science and Technology (CREST), Japan Science and Technology Agency, Tokyo, Japan

Abstract

Cellular senescence is post-mitotic or oncogene-induced events combined with nuclear remodeling. MCAF1 (also known as hAM or ATF7IP), a transcriptional cofactor that is overexpressed in various cancers, functions in gene activation or repression, depending on interacting partners. In this study, we found that MCAF1 localizes to PML nuclear bodies in human fibroblasts and non-cancerous cells. Interestingly, depletion of MCAF1 in fibroblasts induced premature senescence that was characterized by cell cycle arrest, SA-β-gal activity, and senescence-associated heterochromatic foci (SAHF) formation. Under this condition, core histones and the linker histone H1 significantly decreased at both mRNA and protein levels, resulting in reduced nucleosome formation. Consistently, in activated Ras-induced senescent fibroblasts, the accumulation of MCAF1 in PML bodies was enhanced via the binding of this protein to SUMO molecules, suggesting that sequestration of MCAF1 to PML bodies promotes cellular senescence. Collectively, these results reveal that MCAF1 is an essential regulator of cellular senescence.

Citation: Sasai N, Saitoh N, Saitoh H, Nakao M (2013) The Transcriptional Cofactor MCAF1/ATF7IP Is Involved in Histone Gene Expression and Cellular Senescence. PLoS ONE 8(7): e68478. doi:10.1371/journal.pone.0068478

Editor: Joao P.B. Viola, National Cancer Institute (INCA), Brazil

Received March 23, 2013; **Accepted** May 31, 2013; **Published** July 30, 2013

Funding: This work was supported by grants from the Ministry of Education, Culture, Sports, Science and Technology of Japan, and from the Japan Science and Technology Agency (CREST). The funders had no role in study design, data collection and analysis, decision to publish, or preparation of the manuscript.

Competing interests: The authors have declared that no competing interests exist.

* E-mail: mnakao@gpo.kumamoto-u.ac.jp

Introduction

Cellular senescence is a permanent cell cycle arrest that is induced by various stresses such as activated oncogenes, short telomeres, oxidative stress, and inadequate growth conditions [1]. In vivo evidence revealed that cellular senescence occurs in benign or premalignant lesions and acts as an important anti-tumor mechanism [2,3]. Senescent cells are characterized by several features including permanent cell cycle arrest, senescence-associated β-galactosidase (SA-β-gal) activity, morphological changes, activation of DNA damage signaling, and expression of cytokines or secreted factors [1]. Dynamic chromatin changes, including the formation of senescence-associated heterochromatin foci (SAHF), are also observed in senescent cells. The condensed chromatin in senescent cells contributes to the stable repression of proliferation-promoting genes [4]. Increasing number of proteins have been reported to be involved in the chromatin changes during the senescence process [5]. However, little is known about how the epigenetic factors are involved in and contribute to the senescence pathway.

MCAF1 (also known as hAM or ATF7IP) is a transcriptional cofactor that was originally identified as a binding protein of the transcription factor ATF7 [6]. In addition, MCAF1 associates with general transcription factors [6], RNA polymerase II [6,7], and a transcriptional activator SP1 [8]. While MCAF1 associates with the transcriptional apparatus, it also interacts with a methyl-CpG binding protein MBD1 and a H3K9 methyltransferase SETDB1 to form heterochromatin [9,10], suggesting that MCAF1 may function as both a transcriptional activator and a repressor depending on the situation. Biochemical analysis revealed that MCAF1 is an enzymatic cofactor of SETDB1. SETDB1 itself has ability to mono- and di-methylates H3K9, but in the presence of MCAF1 it can also tri-methylate H3K9 [9]. In the cancer cell line C33a, MCAF1, MBD1, and SETDB1 co-localize at the H3K9me3-containing heterochromatin region [8,11]. MCAF1 contains the SUMO-interacting motif (SIM) which preferentially binds to SUMO2/3 [12]. Modification of MBD1 with SUMO2/3 is considered to be required for the recruitment of the MCAF1/SETDB1 complex to DNA-methylated loci to form heterochromatin [11]. Although MCAF1 is overexpressed in various types of cancers [7], the biological significance of MCAF1 remains largely unknown.

Here, we find that, in the human primary diploid fibroblasts IMR90, MCAF1 localizes to PML bodies, but not to H3K9me3-containing heterochromatin. We demonstrate that siRNA-mediated knockdown of MCAF1 in IMR90 cells induces premature senescence. MCAF1 knockdown activates the expression of the cdk inhibitors p16 and p21, dephosphorylates RB, and represses a subset of cell cycle genes. Moreover, core histones and the linker histone H1 are downregulated at both mRNA and protein levels in MCAF1-depleted cells. During senescence induction by activated Ras, the MCAF1 protein level is constant. However, MCAF1 further accumulates in PML bodies in senescent cells by binding to SUMO2/3 through the SIM, implying that sequestration of MCAF1 to PML bodies is necessary for the cells to enter the senescent state. Taken together, these data suggest that MCAF1 is an important regulator of cellular senescence whose activity may be regulated by SUMO.

Material and Methods

Cell culture

IMR90 cells were purchased from ATCC (catalog no. CCL-186) and cultured in DMEM supplemented with 10% FBS. For senescence induction, IMR90 ER: Ras cells [13] were treated with 100 nM 4-hydryoxytamoxifen (4-OHT) for 6 days.

Plasmids, siRNAs, and transfection

The cDNA for wild type and D968A mutant of MCAF1 were inserted into the episomal vector pEBMulti (Wako) together with monomeric EGFP. Plasmid DNAs were transfected with Fugene HD (Roche) for 48 hr.

siRNAs used are Flexitube siRNA (SI04249455 for MCAF1-1, Qiagen), and SMART pool ON-TARGET plus (J-019289-05, J-019289-06, J-019289-07, J-019289-08 for MCAF1-2, Thermoscientific). The siRNA targeted to luciferase (GL3) was used as a control [7]. The siRNAs (2.5 nM) were transfected with the RNAiMAX transfection reagent (Life technologies) every 3 days.

SA-β-gal assay and EdU incorporation assay

SA-β-gal assay was performed using the Senescence Detection Kit (BioVision). For EdU incorporation assay, Click-iT EdU Alexa Fluor 488 Imaging kit was used (Life technologies). EdU incorporation was carried out for 1 hr at 37°C at a final concentration of 10 μM EdU.

Immunofluorescence

Cells were fixed with 4% paraformaldehyde in PBS for 10 min at room temperature and permeabilized with 0.2% triton X-100 in PBS for 5 min on ice. After blocking with 0.5% BSA in PBS for 30 min at R.T, the cells were sequentially incubated with a primary antibody followed by an appropriate secondary antibody. DNA was stained with DAPI and the cells were mounted under coverslips. The cells were analyzed using an Olympus IX71 microscope and the Lumina Vision software. Primary antibodies used are anti-MCAF1 [10], anti-PML (PG-M3, Santa cruz), anti-SUMO2/3 (3H2) [11], anti-macroH2A (39594, Active motif), anti-GFP (A11122, Life technologies), and anti-H3K9me3 (2F3) [14].

RT-qPCR

Total RNA was extracted from cells with TRIzol reagent (Life technologies). RT reaction was carried out with the ReverTraAce qPCR RT kit (Toyobo). For analyzing histone gene expression, total RNA was treated with DNase I (Takara bio) before the RT reaction. qPCR analysis was performed using Thunderbird SYBR qPCR mix (Toyobo) and an ABI Prism 7500 system. Each experiment was carried out at least three times. The fold relative enrichment was quantified, together with normalization by the GAPDH level. Primer sequences used in this study are listed in Supplemental Table **S1**.

Western blot analysis

Total cell lysate was prepared by directly suspending the cells in SDS sample buffer containing benzonase (Sigma). Antibodies used are anti-MCAF1 [10], anti-β-tubulin (T4026, Sigma), anti-p16 (JC8, Santa cruz), anti-p21 (C-19, Sancta cruz), anti-RB (554136, BD), anti-H1 (61202, Active motif), anti-H3 (ab1791, abcam), anti-H2A (39592, Active motif), anti-macroH2A (39594, Active motif), anti-HRas (F235, Santa cruz), and anti-GFP (A11122, Life technologies). Quantification of bands was done with the ImageQuant TL software (GE Healthcare). The band intensities were shown relative to the control, which was normalized to 1.

MNase digestion assay

Extracted nuclei were suspended in MNase buffer (50 mM Tris-HCl pH 7.4, 320 mM sucrose, 4 mM $MgCl_2$, and 1 mM $CaCl_2$) and incubated with MNase (Takara bio) for the indicated times. The reaction was stopped with 10 mM EGTA. Extracted DNA was analyzed by agarose gel electrophoresis.

Microarray and gene set enrichment analysis (GSEA)

Gene expression microarray of total RNA from control or MCAF1-1 siRNA treated cells was performed by Dragon Genomics Center using an Affymetrix GeneChip Human Genome U133 Plus 2.0 array. GSEA was carried out as described [15].

Statistical analyses

Data are presented as means±s.d. All statistical analyses were performed by a two-tailed Student's *t*-test.

Results

MCAF1 localizes to PML bodies in human normal cell lines

To gain insight into the function of MCAF1, we analyzed subcellular localization of MCAF1 in various human cell lines. Immunofluorescence analysis with anti-MCAF1 antibody revealed that MCAF1 displayed two different localization patterns depending on the cell types; heterochromatin and discrete subnuclear foci. As was the case in cancerous C33a

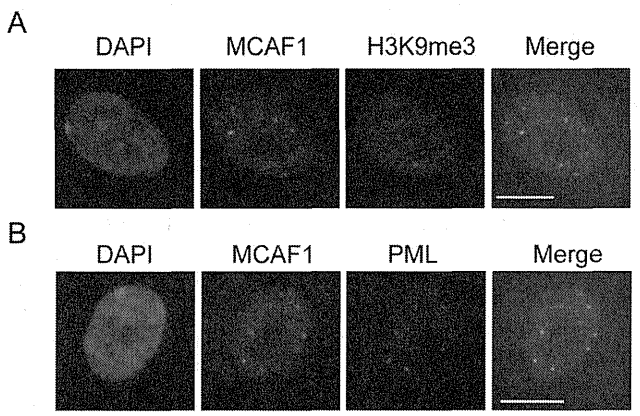

Figure 1. MCAF1 localizes to PML bodies in IMR90 fibroblasts. (**A**) Immunofluorescence analysis of endogenous MCAF1 and H3K9me3 in IMR90 cells. DNA was stained with DAPI. Scale bar: 10 μM. (**B**) Immunofluorescence of endogenous MCAF1 and PML in IMR90 cells. Scale bar: 10 μM.

doi: 10.1371/journal.pone.0068478.g001

cells [11], MCAF1 colocalized with a heterochromatin marker H3K9me3 in HeLa and MCF7 cells (Figure **S1A**). In contrast, in human normal fibroblasts IMR90 and primary mammary epithelial cells HMEC, MCAF1 formed 10-20 discrete nuclear foci that do not accumulate H3K9me3 (Figure **1A**). Co-immunostaining analysis identified these foci as PML nuclear bodies (Figure **1B** and Figure **S1B**). MCAF1 and PML colocalization was not observed in HeLa cells (Figure **S1B**). PML bodies include various proteins involved in transcription, DNA repair, and cellular senescence, and SUMOylation is considered to be essential for the assembly of PML nuclear bodies [16]. MCAF1 does not seem to be a structural component of PML bodies, since MCAF1 knockdown did not affect PML body formation (Figure **S1C**).

MCAF1 knockdown induces cell cycle arrest

To examine the function of MCAF1 in PML bodies, we treated IMR90 cells with two independent siRNAs specific for MCAF1. Knockdown of MCAF1 protein was confirmed at 48 hr after siRNA treatment by Western blot analysis (Figure **2A**). MCAF1 knockdown severely impaired cell proliferation (Figure **2B**) and reduced incorporation of a thymidine analog EdU (Figure **2C**). As MCAF1 is a transcriptional regulator, we sought to identify target genes of MCAF1 by microarray analysis. IMR90 cells were treated with control or MCAF1 siRNAs for 48 hr, total RNA was extracted, and gene expression patterns were compared between control and MCAF1 knockdown cells by microarray and the gene set enrichment analysis. The results show that cell cycle genes were significantly downregulated in MCAF1 knockdown cells (Figure **S2**). To independently confirm the results, we performed RT-qPCR analysis. Again, the cell cycle genes, such as E2F1, MCMs, and CDK1, were significantly decreased by both siRNAs for MCAF1 (Figure **2D**), indicating that a subset of cell cycle genes are downstream targets of MCAF1 in IMR90 cells.

Knockdown of MCAF1 induces premature senescence

We also found that the cdk inhibitors p16 and p21 were upregulated at both mRNA and protein levels (Figure 3**A** and **S3**), and RB protein was dephosphorylated in MCAF1 knockdown cells (Figure **3A**). As cdk inhibitors play important roles in cellular senescence [17], we investigated if MCAF1 knockdown induced premature senescence. As shown in Figure **3B**, MCAF1 knockdown cells were positive for SA-β-gal activity. To further confirm that MCAF1 depletion induced senescence, we tested the formation of SAHF in MCAF1 knockdown cells. DAPI staining showed that approximately 30% of MCAF1 knockdown cells displayed nuclear foci that resemble SAHF (Figure **3C**). SAHF are facultative heterochromatin that is enriched for heterochromatin markers such as H3K9me3, HP1, and macroH2A [5]. The SAHF-like structure in MCAF1 knockdown cells were positive for macroH2A (Figure **3D**) and H3K9me3 (Figure **S4**), indicating that MCAF1 depletion induced SAHF formation. Collectively, these results indicate that MCAF1 knockdown activates the Rb pathway to trigger premature senescence.

Reduction of histone gene expression in MCAF1 knockdown cells

We further investigated the mechanism by which MCAF1 knockdown induces premature senescence. As MCAF1 regulates chromatin state by associating with various proteins, we tested whether chromatin structure is affected in MCAF1 knockdown cells by micrococcal nuclease (MNase) digestion assay. Cell nuclei were collected from control and MCAF1 knockdown cells at 4 days after siRNA treatment. After the nuclei were treated with MNase, DNA was extracted and analyzed by agarose gel electrophoresis. As shown in Figure **4A**, in control cells, MNase digestion generated nucleosome ladders (Figure **4A**, left). Interestingly, in MCAF1 knockdown cells, MNase digestion produced fewer nucleosomes compared to control cells (Figure **4A**, right). As the reduction of undigested DNA in MCAF1 knockdown cells was comparable to that in control cells, these results suggest that the amount of nucleosomes is reduced in MCAF1 knockdown cells.

We then tested the levels of histone proteins in MCAF1 knockdown cells at 8 days after siRNA treatment. The CBB staining after SDS-PAGE showed that the levels of core histone proteins in MCAF1-depleted cells were decreased compared to control cells (Figure **4B**). Western blot analysis also showed that the amount of the core histones H2A and H3 and the linker histone H1 were significantly diminished in MCAF1 knockdown cells (Figure **4C**). However, the variant histone macroH2A was slightly increased in MCAF1 knockdown cells (Figure **4C**), which is consistent with the fact that macroH2A is upregulated in senescent cells [18]. To next investigate whether histone genes are downregulated at a transcriptional level, using RT-qPCR analysis, we analyzed the expression of total 9 histone genes from the histone gene cluster on chromosome 1 (Figure **S5A**). The expression of 8 out of 9 histone genes was downregulated in MCAF1-depleted

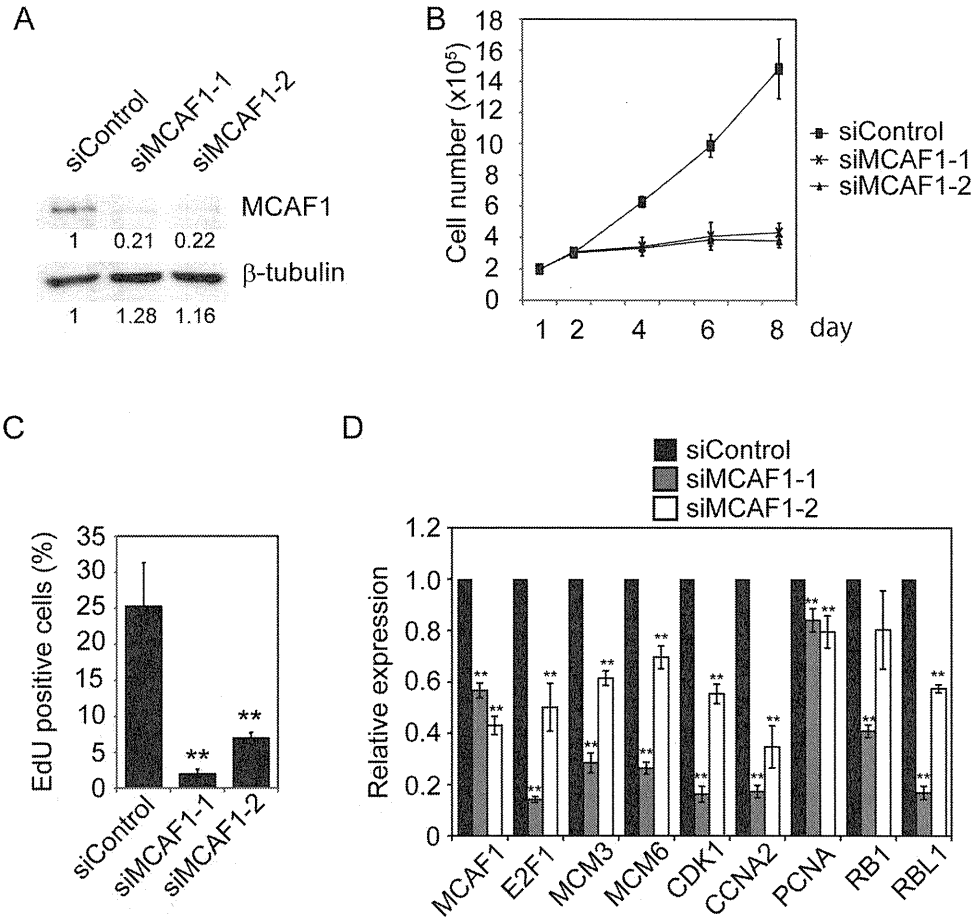

Figure 2. MCAF1 knockdown induces cell cycle arrest. (**A**) IMR90 cells were treated with the indicated siRNAs for 48 hr and analyzed by Western blotting with anti-MCAF1 and anti-β-tubulin antibodies. The images were quantitatively assessed by densitometry. (**B**) Growth curves for siControl, siMCAF1-1, and siMCAF1-2 cells. (**C**) EdU incorporation assay in control and MCAF1 knockdown cells. **P<0.01. (D) RT-qPCR analysis of the cell cycle genes at 48 hr after siRNA treatment. **P<0.01.

doi: 10.1371/journal.pone.0068478.g002

cells at 48 hr after siRNA treatment. The expression of the variant histone genes macroH2A and H3.3A, which are not located on the histone gene cluster, were not decreased by MCAF1 knockdown (Figure **S5B**). These results suggest that histone genes in the histone gene cluster are simultaneously regulated by MCAF1.

MCAF1 localizes to PML bodies through binding to SUMO2/3

As MCAF1 depletion induces premature senescence, we then addressed whether MCAF1 protein level decreases during the senescence process. We induced senescence by expression of 4-OHT-inducible activated Ras (H-RasV12) [13]. Western blot analysis showed that the total amount of MCAF1 protein was constant until day 6 after 4-OHT treatment when cells became fully senescent (Figure **5A**). However, immunofluorescence analysis showed that MCAF1 was further accumulated in PML bodies in SAHF-positive senescent cells compared to in control cells (Figure **5B** and quantitatively shown in Figure **S6**). Similarly, MCAF1 accumulated to PML bodies in replicatively senescent cells (Figure **S7**), suggesting that accumulation of MCAF1 in PML body is a general feature of senescent cells.

We then investigated the mechanism by which MCAF1 is recruited to PML bodies. SUMO2/3 are also known to be accumulated in PML bodies in senescent cells (Figure **S8A**) [19]. As MCAF1 interacts with SUMO2/3 through the SIM [11], it was supposed that MCAF1 is recruited to PML bodies through binding to SUMO2/3. To address this possibility, we expressed EGFP-tagged wild type and the SIM mutant (D968A) [11] of MCAF1 in IMR90 cells and analyzed their localization by immunofluorescence analysis with anti-GFP antibody (Figure **S8B**). The wild type MCAF1 clearly colocalized with PML in transfected cells. In contrast, the SIM mutant of MCAF1 showed diffuse nuclear distribution, although very weak localization in PML bodies was observed (Figure **5C**). These results suggest that the SUMO2/3 binding through

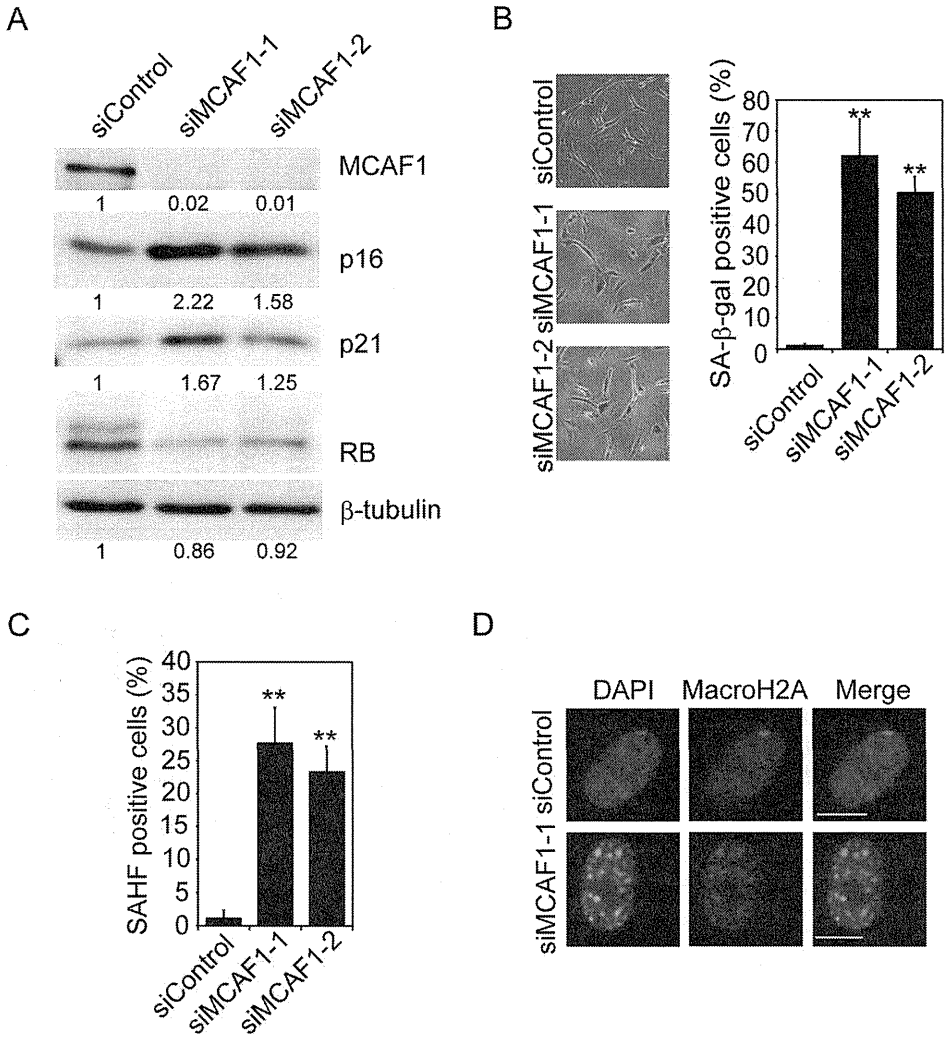

Figure 3. Knockdown of MCAF1 induces premature senescence. (**A**) Western blot analysis of the cdk inhibitors p16 and p21 and RB proteins in control and MCAF1 knockdown IMR90 cells. The images were quantitatively assessed by densitometry. (**B**, **C**) IMR90 cells were treated with the indicated siRNAs, and analyzed for SA-β-gal activity (B) or the formation of SAHF (C) at 8 days after siRNA treatment. **P<0.01. (**D**) Immunofluorescence analysis of MCAF1 and MacroH2A in control and SAHF-positive MCAF1 knockdown cells. DNA was stained with DAPI. Scale bar: 10 μM.

doi: 10.1371/journal.pone.0068478.g003

the SIM is required for the PML body localization of MCAF1 in senescent cells.

Discussion

In this report, we demonstrated that MCAF1 is involved in the regulation of cellular senescence in human primary fibroblast cells. Our data suggest that two factors are major causative for the senescent phenotypes in MCAF1 knockdown cells; the upregulation of the cdk inhibitors and the downregulation of the histone proteins. The cdk inhibitors p16 and p21, which are upregulated in MCAF1 knockdown cells, play important roles in cellular senescence by dephosphorylating RB to repress expression of cell cycle genes [1]. Overexpression of p16 or p21 has been shown to be sufficient to induce senescent phenotypes in fibroblasts [17]. Therefore, upregulation of these cdk inhibitors may be a major factor that triggered senescence in MCAF1 knockdown cells. Further study would be necessary to elucidate which upstream factors activate p16 and p21 in MCAF1 knockdown cells.

Histone protein levels are also associated with the senescence pathway. Core histones and the liker histone H1 are known to be decreased in senescent human cells [18,20,21]. However, it remains unclear whether the histone reduction in MCAF1 knockdown cells is a cause or a result of senescence. It has been reported that histone reduction in yeast shortened lifespan [22]. In addition, depletion of the specific histone H1 variant in cancer cells results in cell cycle

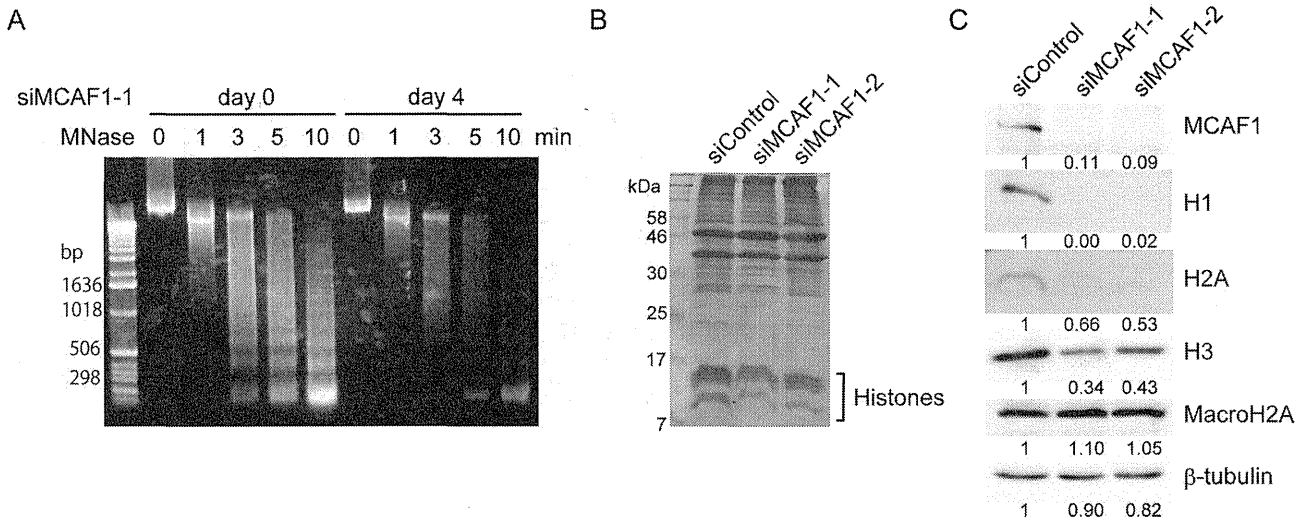

Figure 4. Histones are decreased at both mRNA and protein levels in MCAF1 knockdown cells. (**A**) Nuclei from control and MCAF1 knockdown IMR90 cells at 4 days after siRNA treatment were digested with MNase for the indicated times and analyzed by agarose gel electrophoresis. (**B**) Triton-insoluble fraction at 8 day after siRNA treatment was analyzed by SDS-page followed by CBB staining. (**C**) Western blot analysis of total cell lysates from the indicated cells at 8 days after siRNA treatment. The images were quantitatively assessed by densitometry.

doi: 10.1371/journal.pone.0068478.g004

arrest [23]. Furthermore, knockdown of the histone variants H2AZ or CENPA induces premature senescence [24,25]. Therefore, these findings suggest that histone reduction in MCAF1 knockdown cells may also be causative for the senescence phenotypes.

MCAF1 is a transcriptional cofactor that associates with various proteins involved in transcriptional regulation. However, very few target genes of MCAF1 has been identified so far. We have reported that MCAF1 is required for cancer cell proliferation by activating the transcription of the telomerase genes, TERT and TERC [7]. ChIP-seq analysis in melanoma cells identified the HoxA gene cluster as direct MCAF1 targets [26]. The ChIP-seq data also shows the enrichment of MCAF1 at the histone gene loci and a subset of cell cycle genes, which we showed as possible downstream targets of MCAF1. Therefore, it would be likely that the cell cycle and histone genes are direct transcriptional targets of MCAF1 that are necessary to maintain cell proliferation.

MCAF1 colocalizes with SETDB1 in PML bodies (data not shown), but not with H3K9me3 in IMR90 cells (Figure **1**). Several recent reports demonstrate the PML body localization of SETDB1 in ES cells and in early embryos [27,28]. Our preliminary data suggest that SETDB1 knockdown induces premature senescence. Conversely, SETDB1 is an oncogene whose overexpression in zebra fish abrogates the BRAF(V600E)-induced senescence [26]. Therefore, SETDB1 protein level is also correlated with cell proliferation and senescence in a similar manner with MCAF1. It remains to be elucidated whether the function of the MCAF1/SETDB1 complex in PML bodies is separable from that in heterochromatin in cancer cells. A recent study indicated that the global pattern of H3K9me3 unchanges upon SAHF formation during oncogene-induced senescence, but 3D repositioning of H3K9me3 is involved [29]. In addition, MCAF1 is not required to maintain the H3K9me3 level within SAHF structure (Figure **S4**). Therefore, MCAF1 and SETDB1-mediated H3K9 methylation is not likely to play major roles during the senescence program.

PML protein plays important roles in the senescence pathway through the p53 signaling, and overexpression of PML induces premature senescence [30,31]. The histone chaperon HIRA accumulates in PML bodies in senescent cells similarly to MCAF1, whereas HP1 localizes to PML bodies at earlier stages of senescence before entering SAHF [32]. How dynamic relocalization of the proteins contributes to the senescence remains largely unknown. As both knockdown and PML body recruitment of MCAF1 are connected with the same senescent phenotypes, sequestration of MCAF1 to PML bodies may be essential to inhibit MCAF1 function to activate transcription of cell cycle and histone genes during the senescence pathway (Figure **5D**). SUMO proteins seem to play important roles in this process. Overexpression of SUMO or the SUMO E3 ligase PIA, Sy, or knockdown of the SUMO isopeptidase SENP1 induced senescent-like phenotypes [19,33,34]. Our data show that SUMO2/3 appear to be required for the accumulation of MCAF1 in PML bodies. In cancer cells, MCAF1 is recruited to heterochromatin via the SIM through binding to SUMOylated MBD1 [11]. In senescent cells, there would be some candidates including PML protein itself, which are SUMOylated and recruit MCAF1 to the bodies.

To summarize, our data show that MCAF1 regulates expression of cell cycle and histone genes to maintain cell proliferation, and its inhibition or sequestration to PML bodies are connected with cellular senescence. Given that MCAF1 is

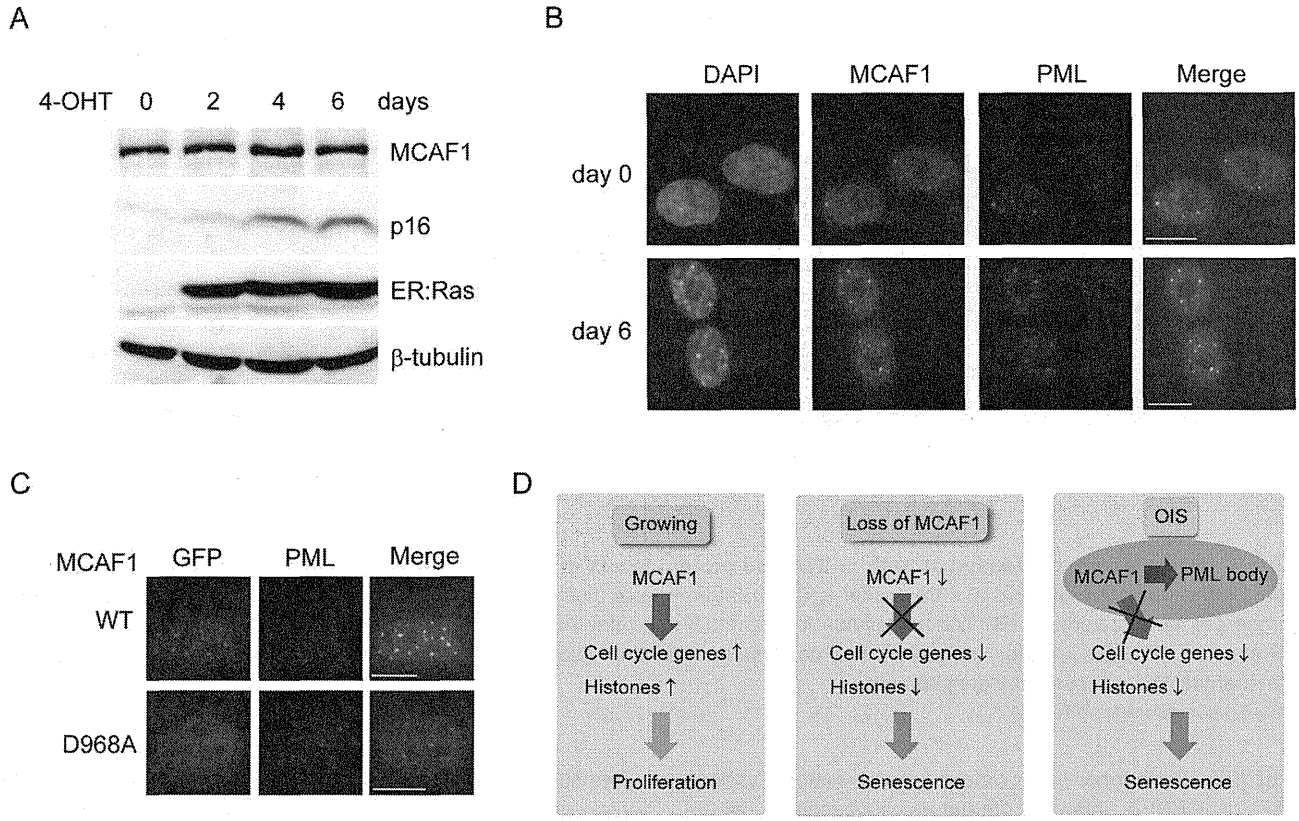

Figure 5. MCAF1 localizes to PML bodies through binding to SUMO2/3. (**A**) Western blot analysis of total cell lysates at the indicated times after ER: Ras induction. (**B**) Immunofluorescence analysis of MCAF1 and PML at 0 and 6 days after ER: Ras induction. Scale bar: 10 μM. (**C**) Immunofluorescence analysis of WT and D968 mutant of MCAF1 with anti-GFP antibody in IMR90 cells. Scale bar: 10 μM. (**D**) Role of MCAF1 in cellular senescence. In growing cells, MCAF1 maintains cell proliferation by activating transcription of cell cycle and histone genes (left). MCAF1 knockdown downregulates cell cycle and histone genes, and results in premature senescence (middle). In oncogene-induced senescent (OIS) cells, MCAF1 is recruited to PML bodies through binding to SUMO2/3. This may inhibit MCAF1 function to maintain expression of cell cycle genes and histones (right).
doi: 10.1371/journal.pone.0068478.g005

overexpressed in various cancers, manipulation of MCAF1 activity or its localization would be a useful tool for anti-cancer therapy.

Supporting Information

Figure S1. MCAF1 localizes to PML bodies in normal cells, but not in cancer cells. (**A**) Immunofluorescence analysis of MCAF1 and a heterochromatin marker H3K9me3 in the cancer cell lines HeLa and MCF7. (**B**) Immunofluorescence of MCAF1 and PML in the normal mammary epithelial cell line HMEC. (**C**) IMR90 cells were treated with siRNA against MCAF1 for 48 hr and analyzed by immunofluorescence with MCAF1 and PML antibodies.
(PDF)

Figure S2. Identification of cell cycle genes as MCAF1 targets by microarray analysis. (**A**) Gene set enrichment analysis was performed to identify gene sets which were downregulated in MCAF1 knockdown cells compared to control cells. A list of top 20 gene sets is shown. Majority of the gene sets downregulated by MCAF1 knockdown are related to the cell cycle process. (**B**) Representative results of GSEA of downregulated genes in MCAF1 knockdown cells.
(PDF)

Figure S3. The cdk inhibitors p16 and p21 are upregulated in MCAF1 knockdown cells. RT-qPCR analysis of p16 and p21 in control and MCAF1 knockdown cells at 2 days after siRNA treatment.
(PDF)

Figure S4. SAHF in MCAF1 knockdown cells are enriched for H3K9me3. Immunofluorescence analysis of MCAF1 and H3K9me3 in control and SAHF-positive MCAF1 knockdown cells.
(PDF)

Figure S5. The core histone and H1 genes are downregulated in MCAF1 knockdown cells. (**A**) RT-qPCR was performed to analyze expression of histone genes in control and MCAF1 knockdown cells at 48 hr after siRNA treatment. (**B**) RT-qPCR analysis of the variant histone genes H3.3A and macroH2A at 48 hr after siRNA treatment.
(PDF)

Figure S6. MCAF1 accumulates in PML body in Ras-induced senescent cells. Line-scan histograms of MCAF1 (green), PML (red), and DAPI (blue) in control (left) and Ras-induced senescent (right) cells. Note that the signal intensity of MCAF1 within PML body in the Ras-induced senescent cells is higher than that in control cells.
(PDF)

Figure S7. MCAF1 is accumulated in PML bodies in replicatively senescent cells. Old IMR90 cells which display SAHF were immunostained with antibodies against MCAF1 and PML.
(PDF)

Figure S8. SUMO2/3 are accumulated in senescent cells. (A) Immunofluorescence of SUMO2/3 and PML at 0 and 6 days after ER: Ras induction. (**B**) Western blot analysis to confirm the expression of monomeric EGFP-tagged wild type and the D968A mutant of MCAF1 in IMR90 cells.
(PDF)

Table S1. A list of primers used in this study. (DOC)

Acknowledgements

We would like to thank Drs. H. Kimura (Osaka University) for antibody against H3K9me3, M. Narita (University of Cambridge) for ER: Ras fibroblasts, and our laboratory members for discussions and technical supports.

Author Contributions

Conceived and designed the experiments: N. Sasai MN. Performed the experiments: N. Sasai MN. Analyzed the data: N. Sasai MN. Contributed reagents/materials/analysis tools: N. Saitoh HS. Wrote the manuscript: N. Sasai MN.

References

1. Kuilman T, Michaloglou C, Mooi WJ, Peeper DS (2010) The essence of senescence. Genes Dev 24: 2463-2479. doi:10.1101/gad.1971610. PubMed: 21078816.
2. Michaloglou C, Vredeveld LC, Soengas MS, Denoyelle C, Kuilman T et al. (2005) BRAFE600-associated senescence-like cell cycle arrest of human naevi. Nature 436: 720-724. doi:10.1038/nature03890. PubMed: 16079850.
3. Braig M, Lee S, Loddenkemper C, Rudolph C, Peters AH et al. (2005) Oncogene-induced senescence as an initial barrier in lymphoma development. Nature 436: 660-665. doi:10.1038/nature03841. PubMed: 16079837.
4. Narita M, Nũnez S, Heard E, Lin AW, Hearn SA et al. (2003) Rb-mediated heterochromatin formation and silencing of E2F target genes during cellular senescence. Cell 113: 703-716. doi:10.1016/S0092-8674(03)00401-X. PubMed: 12809602.
5. Rai TS, Adams PD (2012) Lessons from senescence: Chromatin maintenance in non-proliferating cells. Biochim Biophys Acta 1819: 322-331. doi:10.1016/j.bbagrm.2011.07.014. PubMed: 21839870.
6. De Graeve F, Bahr A, Chatton B, Kedinger C (2000) A murine ATFa-associated factor with transcriptional repressing activity. Oncogene 19: 1807-1819. doi:10.1038/sj.onc.1203492. PubMed: 10777215.
7. Liu L, Ishihara K, Ichimura T, Fujita N, Hino S et al. (2009) MCAF1/AM is involved in Sp1-mediated maintenance of cancer-associated telomerase activity. J Biol Chem 284: 5165-5174. PubMed: 19106100.
8. Ichimura T, Watanabe S, Sakamoto Y, Aoto T, Fujita N et al. (2005) Transcriptional repression and heterochromatin formation by MBD1 and MCAF/AM family proteins. J Biol Chem 280: 13928-13935. doi:10.1074/jbc.M413654200. PubMed: 15691849.
9. Wang H, An W, Cao R, Xia L, Erdjument-Bromage H et al. (2003) mAM facilitates conversion by ESET of dimethyl to trimethyl lysine 9 of histone H3 to cause transcriptional repression. Mol Cell 12: 475-487. doi:10.1016/j.molcel.2003.08.007. PubMed: 14536086.
10. Fujita N, Watanabe S, Ichimura T, Ohkuma Y, Chiba T et al. (2003) MCAF mediates MBD1-dependent transcriptional repression. Mol Cell Biol 23: 2834-2843. doi:10.1128/MCB.23.8.2834-2843.2003. PubMed: 12665582.
11. Uchimura Y, Ichimura T, Uwada J, Tachibana T, Sugahara S et al. (2006) Involvement of SUMO modification in MBD1- and MCAF1-mediated heterochromatin formation. J Biol Chem 281: 23180-23190. doi:10.1074/jbc.M602280200. PubMed: 16757475.
12. Sekiyama N, Ikegami T, Yamane T, Ikeguchi M, Uchimura Y et al. (2008) Structure of the small ubiquitin-like modifier (SUMO)-interacting motif of MBD1-containing chromatin-associated factor 1 bound to SUMO-3. J Biol Chem 283: 35966-35975. doi:10.1074/jbc.M802528200. PubMed: 18842587.
13. Young AR, Narita M, Ferreira M, Kirschner K, Sadaie M et al. (2009) Autophagy mediates the mitotic senescence transition. Genes Dev 23: 798-803. doi:10.1101/gad.519709. PubMed: 19279323.
14. Hayashi-Takanaka Y, Yamagata K, Wakayama T, Stasevich TJ, Kainuma T et al. (2011) Tracking epigenetic histone modifications in single cells using Fab-based live endogenous modification labeling. Nucleic Acids Res 39: 6475-6488. doi:10.1093/nar/gkr343. PubMed: 21576221.
15. Subramanian A, Tamayo P, Mootha VK, Mukherjee S, Ebert BL et al. (2005) Gene set enrichment analysis: a knowledge-based approach for interpreting genome-wide expression profiles. Proc Natl Acad Sci U S A 102: 15545-15550. doi:10.1073/pnas.0506580102. PubMed: 16199517.
16. Bernardi R, Pandolfi PP (2007) Structure, dynamics and functions of promyelocytic leukaemia nuclear bodies. Nat Rev Mol Cell Biol 8: 1006-1016. doi:10.1038/nrm2277. PubMed: 17928811.
17. McConnell BB, Starborg M, Brookes S, Peters G (1998) Inhibitors of cyclin-dependent kinases induce features of replicative senescence in early passage human diploid fibroblasts. Curr Biol 8: 351-354. doi:10.1016/S0960-9822(98)70137-X. PubMed: 9512419.
18. Sporn JC, Kustatscher G, Hothorn T, Collado M, Serrano M et al. (2009) Histone macroH2A isoforms predict the risk of lung cancer recurrence. Oncogene 28: 3423-3428. doi:10.1038/onc.2009.26. PubMed: 19648962.
19. Yates KE, Korbel GA, Shtutman M, Roninson IB, DiMaio D (2008) Repression of the SUMO-specific protease Senp1 induces p53-dependent premature senescence in normal human fibroblasts. Aging Cell 7: 609-621. doi:10.1111/j.1474-9726.2008.00411.x. PubMed: 18616636.
20. O'Sullivan RJ, Kubicek S, Schreiber SL, Karlseder J (2010) Reduced histone biosynthesis and chromatin changes arising from a damage signal at telomeres. Nat Struct Mol Biol 17: 1218-1225. doi:10.1038/nsmb.1897. PubMed: 20890289.
21. Funayama R, Saito M, Tanobe H, Ishikawa F (2006) Loss of linker histone H1 in cellular senescence. J Cell Biol 175: 869-880. doi:10.1083/jcb.200604005. PubMed: 17158953.
22. Feser J, Truong D, Das C, Carson JJ, Kieft J et al. (2010) Elevated histone expression promotes life span extension. Mol Cell 39: 724-735. doi:10.1016/j.molcel.2010.08.015. PubMed: 20832724.
23. Sancho M, Diani E, Beato M, Jordan A (2008) Depletion of human histone H1 variants uncovers specific roles in gene expression and cell growth. PLOS Genet 4: e1000227. PubMed: 18927631.
24. Maehara K, Takahashi K, Saitoh S (2010) CENP-A reduction induces a p53-dependent cellular senescence response to protect cells from